

**What happens next and when “next” happens:  
Mechanisms of spatial and temporal prediction**

by

**Dean R. Wyatte**

B.S., Indiana University Bloomington, 2007

M.A., University of Colorado Boulder, 2010

A thesis submitted to the  
Faculty of the Graduate School of the  
University of Colorado in partial fulfillment  
of the requirements for the degree of  
Doctor of Philosophy  
Department of Psychology and Neuroscience  
2014

This thesis entitled:  
What happens next and when “next” happens:  
Mechanisms of spatial and temporal prediction  
written by Dean R. Wyatte  
has been approved for the Department of Psychology and Neuroscience

---

Randall C. O'Reilly

---

Prof. Tim Curran

---

Prof. Albert Kim

Date \_\_\_\_\_

The final copy of this thesis has been examined by the signatories, and we find that both the content and the form meet acceptable presentation standards of scholarly work in the above mentioned discipline.

Wyatte, Dean R. (Ph.D., Cognitive Neuroscience)

What happens next and when “next” happens:

Mechanisms of spatial and temporal prediction

Thesis directed by Prof. Randall C. O'Reilly

## **Acknowledgements**

## **Contents**

### **Chapter**

|                                  |   |           |
|----------------------------------|---|-----------|
| <b>1</b>                         | <b>Introduction</b>   | <b>1</b>  |
|                                  |   |           |
| <b>Bibliography</b>              |   | <b>2</b>  |
| <b>2</b>                         |   | <b>7</b>  |
| 2.1                              | Introduction . . . . .  | 7         |
| 2.2                              | LeabraTI biological details . . . . .                                   | 8         |
| 2.2.1                            | Laminar structure and microcircuitry of the neocortex . . . . .         | 8         |
| 2.2.2                            | Pacemaker properties of Layer 5 and thalamic bursting neurons . . . . . | 11        |
| 2.2.3                            | Summary of LeabraTI computation . . . . .                               | 13        |
| 2.3                              | LeabraTI predictions . . . . .  | 15        |
| 2.3.1                            | Relation to existing models . . . . .                                   | 15        |
| 2.3.2                            | Testable predictions . . . . .  | 15        |
|                                  |   |           |
| <b>Bibliography</b>              |   | <b>16</b> |
| <b>3</b>                         | Spatial and temporal prediction during novel object recognition:        |           |
| Temporal and spectral signatures |   | 20        |
| 3.1                              | Introduction . . . . .  | 20        |
| 3.2                              | Methods . . . . .   | 20        |

|  |    |
|--|----|
| 3.2.1 Participants . . . . .   | 20 |
| 3.2.2 Stimuli . . . . .  | 20 |
| 3.2.3 Procedure . . . . .  | 22 |
| 3.2.4 EEG recording and preprocessing . . . . .  | 24 |
| 3.2.5 Event-related averaging . . . . .  | 25 |
| 3.2.6 Time-frequency analysis . . . . .  | 26 |
| 3.3 Results . . . . .  | 27 |
| 3.3.1 Behavioral measures of spatial and temporal predictability . . . . .                         | 27 |
| 3.3.2 Time course of spatial and temporal predictability . . . . .                                 | 29 |
| 3.3.3 Predictability entrains alpha oscillations . . . . .   | 32 |
| 3.3.4 Predictability effects in delta-theta bands . . . . .  | 33 |
| 3.4 Discussion . . . . .   | 37 |
| 3.4.1 Summary of results . . . . .   | 37 |
| 3.4.2 Separate time courses for spatial and temporal prediction . . . . .                          | 39 |
| 3.4.3 Oscillatory mechanisms of spatial and temporal prediction . . . . .                          | 39 |
| 3.4.4 Prediction is not simply attentional orienting . . . . .                                     | 41 |
| 3.4.5 Why does combined spatial and temporal predictability increase inverse efficiency? . . . . . | 42 |
| <b>Bibliography</b>  | 42 |
| <b>4 Effects of spatial and temporal prediction during novel object learning</b>                   | 46 |
| 4.1 Introduction . . . . .   | 46 |
| 4.2 Methods . . . . .  | 46 |
| 4.2.1 Participants . . . . .   | 46 |
| 4.2.2 Stimuli . . . . .  | 46 |
| 4.2.3 Procedure . . . . .  | 47 |

|                         |   |    |
|-------------------------|---|----|
| 4.3                     | Results . . . . .   | 48 |
| 4.4                     | Discussion . . . . .  | 54 |
| 4.4.1                   | Summary of results . . . . .  | 54 |
| 4.4.2                   | A behavioral disadvantage for spatial prediction during object learning . . | 54 |
| 4.4.3                   | Spatiotemporal prediction biases development of invariance . . . . .        | 55 |
| <br><b>Bibliography</b> |   | 55 |
| <br><b>5</b>            |   | 60 |
| 5.1                     | Introduction . . . . .  | 60 |
| <br><b>Bibliography</b> |   | 60 |
| <br><b>6</b>            | General Discussion  | 64 |
| <br><b>Bibliography</b> |   | 64 |
| <br><b>Bibliography</b> |   | 67 |

## Figures

### Figure

|      |  |    |
|------|--|----|
| 2.1  | The Simple Recurrent Network (SRN) and microcircuitry of the neocortex . . . . . | 9  |
| 2.2  | The LeabraTI model computation. . . . .  | 14 |
| 3.1  | Novel “paper clip” objects . . . . .   | 21 |
| 3.2  | Experimental procedure . . . . .   | 23 |
| 3.3  | Electrode pooling for analyses . . . . .   | 25 |
| 3.4  | Behavioral measures of spatial and temporal predictability . . . . .             | 28 |
| 3.5  | Entrainier-evoked activity . . . . .   | 31 |
| 3.6  | Probe-evoked activity . . . . .  | 32 |
| 3.7  | Effect of entrainer predictability on alpha power . . . . .                      | 34 |
| 3.8  | Effect of entrainer predictability on alpha phase coherence . . . . .            | 35 |
| 3.9  | Alpha phase coherence before and after probe . . . . .                           | 36 |
| 3.10 | Delta-theta power before and after probe . . . . .                               | 36 |
| 3.11 | Delta-theta phase coherence before and after probe . . . . .                     | 37 |
| 4.1  | Novel “paper clip” objects . . . . .   | 47 |
| 4.2  | Experimental procedure . . . . .   | 49 |
| 4.3  | Behavioral measures of spatial and temporal predictability . . . . .             | 50 |
| 4.4  | Behavioral measures for each target object . . . . .                             | 51 |
| 4.5  | Accuracy as a function of viewing angle for each target object . . . . .         | 52 |

|  |    |
|--|----|
| 4.6 Bootstrapped accuracy for degenerate views . . . . . | 53 |
|--|----|

# **Chapter 1**

## **Introduction**

How does the brain predict what happens from one moment to the next? This is an important question in research on perception across all modalities that is surprisingly often overlooked in the fields of psychology and neuroscience. For example, most experiments are designed to measure evoked responses to a randomly chosen, isolated stimulus under the tacit assumption that response variability is irrelevant noise that should be averaged out across many presentations. Computational models of perceptual processing often operate under similar assumptions in which stimuli are presented as random “snapshots” from which some common set of features should be learned to minimize representational variability across presentations (e.g., Serre, Oliva, & Poggio, 2007; Mutch & Lowe, 2008; although see Foldiak, 1991, for a notable exception). These experimental and computational assumptions stand in contrast to the event structure of the physical world, which is deterministic from one moment to the next.

An equally important question is concerned with how the brain knows when to make its next prediction. Predicting what happens next requires integrating information over some time frame and using the result to drive the actual prediction, but when should integration start? And for how long? Perceptual processing has been shown to undergo temporal fluctuations and in extreme cases, stimuli can be rendered imperceptible if presented during one of these fluctuations (Busch, Dubois, & VanRullen, 2009; VanRullen, Busch, Drewes, & Dubois, 2011; Mathewson et al., 2011). Again, many laboratory experiments tend not to be concerned with these temporal fluctuations, as they simply add variability to responses that will average out over a large number

of trials and can be mitigated by design decisions such as using a fixation cross to denote the start of a trial. Computational models, similarly, often completely ignore time altogether, although recent advances in spiking models of perceptual processing (e.g., Masquelier & Thorpe, 2007) are beginning to address this issue.

The goal of the proposed work is to begin systematically investigating the neural mechanisms and circuitry related to prediction and temporal integration. Recently, our lab has developed a theoretical framework and general model for describing how these functions are implemented in the brain. This framework, henceforth referred to as *LeabraTI*,<sup>1</sup> brings together a large number of independent findings from the systems neuroscience literature to describe how multiple interacting mechanisms accomplish prediction and temporal integration in cortex. The fundamental proposal of the LeabraTI theory is that time in the brain is discretized (at least partially) into reference frames that can be associated via general learning mechanisms (e.g., Hebbian and error-driven learning) so that representation of information during one frame can be used to predict what happens during the next. This proposal requires at least two mechanisms: (1.) A mechanism that establishes reference frames over which information is integrated and, (2.) A mechanism that generates the actual prediction itself and validates it against what actually happens.

As will be discussed in detail in Chapter 2, the LeabraTI theory's proposed mechanisms are suggested to be dissociable, generating signatures at distinct spectral frequencies which can be measured physiologically. The potential dissociability of the spatial and temporal components of prediction establishes a number of immediately testable predictions that will form the experimental component of the proposed work.

## References

- Armstrong-James, M., Fox, K., & Das-Gupta, A. (1992). Flow of excitation within rat barrel cortex on striking a single vibrissa. *Journal of Neurophysiology*, 68(4), 1345–1358.

---

<sup>1</sup> Leabra refers to a general model of learning in the neocortex (O'Reilly & Munakata, 2000; O'Reilly, Munakata, Frank, Hazy, & Contributors, 2012); TI to Temporal Integration.

- Arnal, L. H., & Giraud, A.-L. (2012). Cortical oscillations and sensory predictions. *Trends in Cognitive Sciences*, *16*(7), 390–398.
- Balas, B. J., & Sinha, P. (2009). The role of sequence order in determining view canonicality for novel wire-frame objects. *Attention, Perception & Psychophysics*, *71*(4), 712–723.
- Benjamini, Y., & Yekutieli, D. (2001). The control of the false discovery rate in multiple testing under dependency. *The Annals of Statistics*, *29*(4), 1165–1188.
- Brainard, D. (1997). The Psychophysics Toolbox. *Spatial Vision*, *10*(4), 433–436.
- Buffalo, E. A., Fries, P., Landman, R., Buschman, T. J., & Desimone, R. (2011). Laminar differences in gamma and alpha coherence in the ventral stream. *Proceedings of the National Academy of Sciences of the United States of America*, *108*(27), 11262–11267.
- Bulthoff, H. H., & Edelman, S. (1992). Psychophysical support for a two-dimensional view interpolation theory of object recognition. *Proceedings of the National Academy of Sciences of the United States of America*, *89*(1), 60–64.
- Busch, N. A., Dubois, J., & VanRullen, R. (2009). The phase of ongoing EEG oscillations predicts visual perception. *The Journal of Neuroscience*, *29*(24), 7869–7876.
- Buxhoeveden, D. P., & Casanova, M. F. (2002). The minicolumn hypothesis in neuroscience. *Brain*, *125*(Pt 5), 935–951.
- Connors, B. W., Gutnick, M. J., & Prince, D. A. (1982). Electrophysiological properties of neocortical neurons in vitro. *Journal of Neurophysiology*, *48*(6), 1302–1320.
- Cousineau, D. (2005). Confidence intervals in within-subject designs: A simpler solution to Loftus and Massons method. *Tutorials in Quantitative Methods for Psychology*, *1*(1), 42–45.
- Delorme, A., & Makeig, S. (2004). EEGLAB: An open source toolbox for analysis of single-trial EEG dynamics including independent component analysis. *Journal of Neuroscience Methods*, *134*(1), 9–21.
- Doherty, J. R., Rao, A., Mesulam, M. M., & Nobre, A. C. (2005). Synergistic effect of combined temporal and spatial expectations on visual attention. *The Journal of Neuroscience*, *25*(36), 8259–8266.
- Douglas, R. J., & Martin, K. A. C. (2004). Neuronal circuits of the neocortex. *Annual Review of Neuroscience*, *27*, 419–451.
- Edelman, S., & Bulthoff, H. H. (1992). Orientation dependence in the recognition of familiar and novel views of three-dimensional objects. *Vision Research*, *32*(12), 2385–2400.
- Elman, J. L. (1990). Finding structure in time. *Cognitive Science*, *14*(2), 179–211.
- Fahrenfort, J. J., Scholte, H. S., & Lamme, V. A. F. (2007). Masking disrupts reentrant processing in human visual cortex. *Journal of Cognitive Neuroscience*, *19*(9), 1488–1497.
- Felleman, D. J., & Van Essen, D. C. (1991). Distributed hierarchical processing in the primate cerebral cortex. *Cerebral Cortex*, *1*(1), 1–47.
- Foldiak, P. (1991). Learning invariance from transformation sequences. *Neural Computation*, *3*(2), 194–200.

- Franceschetti, S., Guatteo, E., Panzica, F., Sancini, G., Wanke, E., & Avanzini, G. (1995). Ionic mechanisms underlying burst firing in pyramidal neurons: Intracellular study in rat sensorimotor cortex. *Brain Research*, *696*(1–2), 127–139.
- Giraud, A.-L., & Poeppel, D. (2012). Cortical oscillations and speech processing: Emerging computational principles and operations. *Nature Neuroscience*, *15*(4), 511–517.
- Hirsch, J. A., & Martinez, L. M. (2006). Laminar processing in the visual cortical column. *Current Opinion in Neurobiology*, *16*(4), 377–384.
- Horton, J. C., & Adams, D. L. (2005). The cortical column: A structure without a function. *Philosophical Transactions of the Royal Society B*, *360*(1456), 837–862.
- Hubel, D. H., & Wiesel, T. N. (1977). Ferrier lecture. Functional architecture of macaque monkey visual cortex. *Proceedings of the Royal Society B*, *198*(1130), 1–59.
- Hughes, S. W., Lorincz, M., Cope, D. W., Blethyn, K. L., Kekesi, K. A., Parri, H. R., Juhasz, G., & Crunelli, V. (2004). Synchronized oscillations at alpha and theta frequencies in the lateral geniculate nucleus. *Neuron*, *42*(2), 253–268.
- Jones, E. G. (2000). Microcolumns in the cerebral cortex. *Proceedings of the National Academy of Sciences of the United States of America*, *97*(10), 5019–5021.
- Lachaux, J. P., Rodriguez, E., Martinerie, J., & Varela, F. J. (1999). Measuring phase synchrony in brain signals. *Human Brain Mapping*, *8*(4), 194–208.
- Lakatos, P., Karmos, G., Mehta, A. D., Ulbert, I., & Schroeder, C. E. (2008). Entrainment of neuronal oscillations as a mechanism of attentional selection. *Science*, *320*(5872), 110–113.
- Logothetis, N., Pauls, J., Bulthoff, H., & Poggio, T. (1994). View-dependent object recognition by monkeys. *Current Biology*, *4*(5), 401–414.
- Logothetis, N. K., Pauls, J., & Poggio, T. (1995). Shape representation in the inferior temporal cortex of monkeys. *Current Biology*, *5*(5), 552–563.
- Lopes da Silva, F. (1991). Neural mechanisms underlying brain waves: from neural membranes to networks. *Electroencephalography and Clinical Neurophysiology*, *79*(2), 81–93.
- Lorincz, M. L., Crunelli, V., & Hughes, S. W. (2008). Cellular dynamics of cholinergically induced alpha (8–13 hz) rhythms in sensory thalamic nuclei in vitro. *The Journal of Neuroscience*, *28*(3), 660–671.
- Lorincz, M. L., Kekesi, K. A., Juhasz, G., Crunelli, V., & Hughes, S. W. (2009). Temporal framing of thalamic relay-mode firing by phasic inhibition during the alpha rhythm. *Neuron*, *63*(5), 683–696.
- Luczak, A., Bartho, P., & Harris, K. D. (2013). Gating of sensory input by spontaneous cortical activity. *The Journal of Neuroscience*, *33*(4), 1684–1695.
- Lumer, E., Edelman, G., & Tononi, G. (1997). Neural dynamics in a model of the thalamocortical system. I. Layers, loops and the emergence of fast synchronous rhythms. *Cerebral Cortex*, *7*(3), 207–227.
- Masquelier, T., & Thorpe, S. J. (2007). Unsupervised learning of visual features through spike timing dependent plasticity. *PLoS Computational Biology*, *3*(2), 247–257.

- Mathewson, K. E., Lleras, A., Beck, D. M., Fabiani, M., Ro, T., & Gratton, G. (2011). Pulsed out of awareness: EEG alpha oscillations represent a pulsed-inhibition of ongoing cortical processing. *Frontiers in Psychology*, 2.
- Mountcastle, V. B. (1997). The columnar organization of the neocortex. *Brain*, 120(Pt 4), 701–722.
- Mutch, J., & Lowe, D. (2008). Object class recognition and localization using sparse features with limited receptive fields. *International Journal of Computer Vision*, 80(1), 45–57.
- Oostenveld, R., Fries, P., Maris, E., & Schoffelen, J.-M. (2011). FieldTrip: Open source software for advanced analysis of MEG, EEG, and invasive electrophysiological data. *Computational Intelligence and Neuroscience*, 2011.
- O'Reilly, R. C., & Munakata, Y. (2000). *Computational Explorations in Cognitive Neuroscience: Understanding the Mind by Simulating the Brain*. Cambridge, MA: The MIT Press.
- O'Reilly, R. C., Munakata, Y., Frank, M. J., Hazy, T. E., & Contributors (2012). *Computational Cognitive Neuroscience*. Wiki Book, 1st Edition, URL: <http://ccnbook.colorado.edu>.
- Pelli, D. (1997). The VideoToolbox software for visual psychophysics: Transforming numbers into movies. *Spatial Vision*, 10(4), 437–442.
- Perrin, F., Pernier, J., Bertrand, O., & Echallier, J. F. (1989). Spherical splines for scalp potential and current density mapping. *Electroencephalography and Clinical Neurophysiology*, 72(2), 184–187.
- Rockland, K. S., & Pandya, D. N. (1979). Laminar origins and terminations of cortical connections of the occipital lobe in the rhesus monkey. *Brain Research*, 179(1), 3–20.
- Rohenkohl, G., & Nobre, A. C. (2011). Alpha oscillations related to anticipatory attention follow temporal expectations. *The Journal of Neuroscience*, 31(40), 14076–14084.
- Schroeder, C. E., & Lakatos, P. (2009). Low-frequency neuronal oscillations as instruments of sensory selection. *Trends in Neurosciences*, 32(1), 9–18.
- Serre, T., Oliva, A., & Poggio, T. (2007). A feedforward architecture accounts for rapid categorization. *Proceedings of the National Academy of Sciences of the United States of America*, 104(15), 6424–6429.
- Servan-Schreiber, D., Cleeremans, A., & McClelland, J. L. (1991). Graded state machines: The representation of temporal contingencies in simple recurrent networks. *Machine Learning*, 7(2–3), 161–193.
- Silva, L. R., Amitai, Y., & Connors, B. W. (1991). Intrinsic oscillations of neocortex generated by layer 5 pyramidal neurons. *Science*, 251(4992), 432–435.
- Sinha, P., & Poggio, T. (1996). Role of learning in three-dimensional form perception. *Nature*, 384(6608), 460–463.
- Spaak, E., Bonnefond, M., Maier, A., Leopold, D. A., & Jensen, O. (2012). Layer-specific entrainment of gamma-band neural activity by the alpha rhythm in monkey visual cortex. *Current Biology*, 22(24), 2313–2318.

- Stefanics, G., Hangya, B., Herndi, I., Winkler, I., Lakatos, P., & Ulbert, I. (2010). Phase entrainment of human delta oscillations can mediate the effects of expectation on reaction speed. *The Journal of Neuroscience*, 30(41), 13578–13585.
- Thomson, A. M. (2010). Neocortical layer 6, a review. *Frontiers in Neuroanatomy*, 4.
- Thomson, A. M., & Lamy, C. (2007). Functional maps of neocortical local circuitry. *Frontiers in Neuroscience*, 1(1), 19–42.
- Townshend, J. T., & Ashby, F. G. (1983). *Stochastic Modeling of Elementary Psychological Processes*. Cambridge: Cambridge University Press.
- Townshend, J. T., & Ashby, F. G. (2005). Methods of modeling capacity in simple processing systems. In J. N. Castellan Jr., & F. Restle (Eds.), *Cognitive Theory: Volume 3* (pp. 200–239). Hillsdale, NJ: Lawrence Erlbaum Associates.
- VanRullen, R., Busch, N. A., Drewes, J., & Dubois, J. (2011). Ongoing EEG phase as a trial-by-trial predictor of perceptual and attentional variability. *Frontiers in Psychology*, 2.
- Will, U., & Berg, E. (2007). Brain wave synchronization and entrainment to periodic acoustic stimuli. *Neuroscience letters*, 424(1), 55–60.

## **Chapter 2**

### **2.1 Introduction**

The *LeabraTI* framework is a mechanistic description and general model of how prediction and temporal integration might work in the brain. The general idea is closely related to the Simple Recurrent Network (SRN) (Elman, 1990; Servan-Schreiber, Cleeremans, & McClelland, 1991) an artificial neural network architecture that explicitly represents temporally lagged information in discrete “context” units whose activity gets integrated with more current information to predict what happens in the next time step (Figure 2.1a). This method of copying a contextual representation from an intermediate representation at discrete intervals was originally shown to be a robust way to leverage error-driven learning to represent latent temporal structure in auditory streams and artificial grammars. More generally, the SRN’s explicit representation of temporal context can capture the latent structure of any stimulus that varies systematically over time, making it a good basis for a generic prediction and temporal integration mechanism.

However, LeabraTI differs in several key ways from the traditional SRN architecture, primarily in the way temporally lagged context is represented and used in neural processing. These differences are due to biological constraints imposed by the circuitry of the neocortex, and thus form a number of testable predictions that can be used to evaluate the validity of the LeabraTI framework. The central prediction of LeabraTI is that temporal context is updated in a periodic manner, approximately every 100 ms, subserved by deep (Layer 5 and 6) neurons. This periodic updating is suggested to contribute to the brain’s alpha rhythm, which has been studied extensively

using scalp electroencephalography. This chapter **TODO – also need something here about error driven learning**

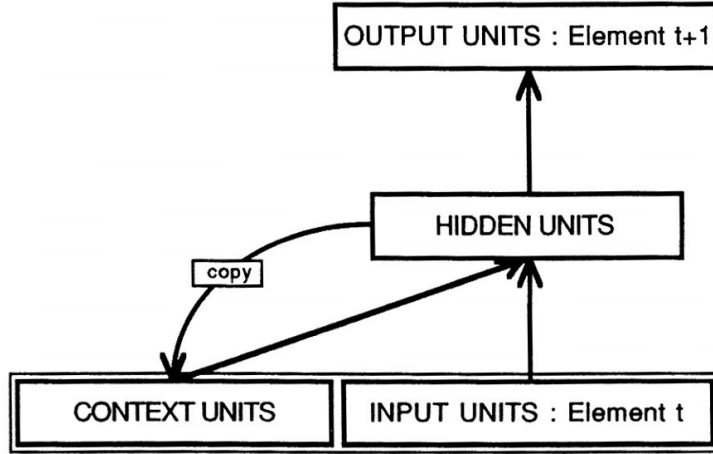
## 2.2 LeabraTI biological details

### 2.2.1 Laminar structure and microcircuitry of the neocortex

A salient feature of the brain, and potential clue in realizing how an SRN-like computation might be carried out in biological neural circuits, is the laminar structure prevalent across the neocortex (Figure 2.1b). Incoming information from the sensory periphery is transmitted through the thalamus and targets Layer 4 neurons in the primary sensory cortices (e.g., V1). From there, Layer 4 neurons propagate spikes to superficial neurons (Layers 2 and 3) which in turn target Layer 4 neurons of higher-level cortices, forming the prominent corticocortical feedforward pathways that subserve visual and auditory recognition (Felleman & Van Essen, 1991). Corticocortical feedback originates in superficial layers or Layer 6 of the higher-level cortex and generally terminates on superficial neurons of the lower-level cortex (Rockland & Pandya, 1979). In addition to these interareal pathways, there exists a canonical microcircuit of the form Layer 4 → Layer 2/3 → Layer 5 → Layer 6 that routes spike propagation through the local neuronal structure (Douglas & Martin, 2004; Thomson & Lamy, 2007). This microcircuit forms the core computational unit of LeabraTI, as will be described in this and the following sections.

The importance of the local microcircuit was first suggested by Vernon Mountcastle in his proposal regarding the gross columnar organization of the neocortex (see Mountcastle, 1997, for a comprehensive review). Mountcastle's proposal states that microcolumns composed of around 80-100 neurons extending vertically through all six lamina with canonical circuitry form the core repeating structure of the neocortex. Neurons within a single microcolumnar circuit possess nearly identical receptive field tunings across lamina while neurons in neighboring microcolumns (radial separation greater than 600 μm) possess very different receptive field tunings but contribute to the higher-order macrocolumn (i.e., hypercolumn) structure (Hubel & Wiesel, 1977; Jones, 2000).

A



B

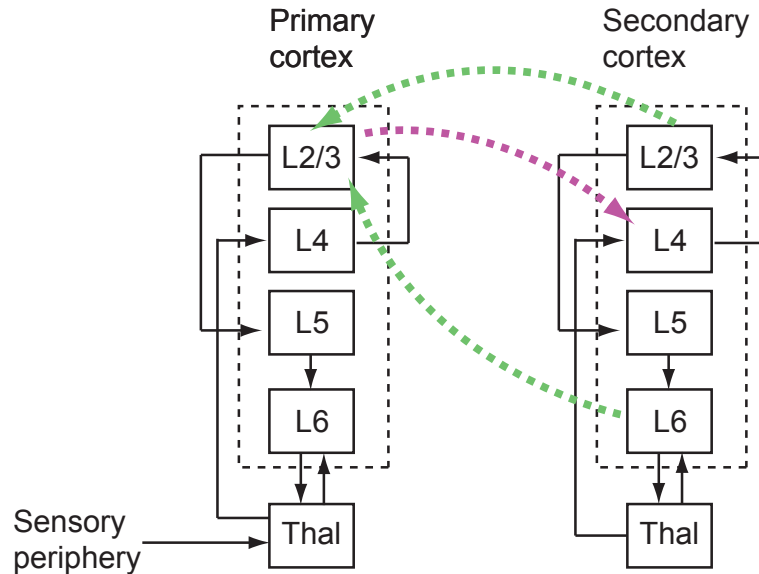


Figure 2.1: The Simple Recurrent Network (SRN) and microcircuitry of the neocortex

**A:** The SRN represents temporal information explicitly using discrete context units that are updated once per time step. Context is integrated with more current inputs to predict information at the subsequent time step. Reproduced from Servan-Schreiber et al. (1991). **B:** The neocortex is laminated with canonical circuitry between neurons across layers and between areas. Intraareal connections are shown in black with interareal feedforward connections in purple and feedback connections in green.

Microcolumns have been identified in a variety of neural systems with this electrophysiological mapping and are also prominently visible under Nissl staining. Despite this evidence for their structural existence, any function of the microcolumn aside from an organizing principle remains debated (Buxhoeveden & Casanova, 2002; Horton & Adams, 2005).

LeabraTI provides a computational role for the microcolumn, by mapping an SRN-like computation onto their Layer 4 → Layer 2/3 → Layer 5 → Layer 6 circuit. In this mapping, superficial neurons continuously integrate feedforward and feedback interareal synapses to process current information. Layer 2/3 → Layer 5 → Layer 6 provides an intraareal pathway for explicitly representing temporal context deep layers, which are relatively isolated from nonlocal inputs. There is also appropriate circuitry for recirculating this context through the local microcolumn via Layer 4 to drive the learning of temporal associations. This basic idea provides a concise explanation for the strong degree of isotuning throughout a single microcolumn, as deep neurons need to represent the same information as superficial neurons except at a delayed interval.

More generally, LeabraTI's dichotomy of continuous integration in superficial layers and periodic updating of deep layers receives strong support by the literature. Recent studies that have employed depth electrodes to simultaneously record from multiple layers within a patch of cortex have indicated that superficial layers exhibit spectral power at much higher frequencies than deep layers. Buffalo, Fries, Landman, Buschman, and Desimone (2011) recorded responses from ventral visual sites V1, V2, and V4 in awake, behaving monkeys during a simple directed attention task, finding a dissociation in spike coherence frequency in superficial (gamma spectrum, peak ~50 Hz) and deep layers (alpha spectrum, peak ~10 Hz). A similar experimental paradigm expands on these findings by demonstrating cross-frequency coupling between gamma and alpha spectra localized to superficial and deep layers, respectively (Spaak, Bonnefond, Maier, Leopold, & Jensen, 2012). The cross-frequency coupling is characterized by a clear nesting of gamma activity within alpha cycles, suggesting that deep neurons' alpha activity might subserve a general pacemaker mechanism. In the context of LeabraTI, this pacemaker property is important to ensure the regular updating of context through deep layers and temporally predictable reintegration with more current

information.

In summary, the laminocolumnar organization of the neocortex provides the dual pathways necessary for continuous information processing and the SRN's explicit temporal context representation. One question that remains, however, concerns the 10 Hz alpha periodicity of deep neurons. The Layer 4 → Layer 2/3 → Layer 5 → Layer 6 microcircuit only contains four synapses including the thalamus and intracolumnar monosynaptic latencies for regular spiking neurons are on the order of 5 ms or faster (Armstrong-James, Fox, & Das-Gupta, 1992; Lumer, Edelman, & Tononi, 1997). This relatively small amount of tissue, if driven with constant input, would cause deep neurons to spike at a rate much faster than 10 Hz. How such a circuit could produce the strong alpha power observed in recent depth recordings is described next.

### **2.2.2 Pacemaker properties of Layer 5 and thalamic bursting neurons**

Layer 5 neurons can be roughly divided into 5a and 5b subtypes (Thomson & Lamy, 2007). Layer 5a neurons have relatively small cell bodies and exhibit “regular spiking” depolarization responses. They collect input from other Layer 5a neurons and pass it to 5b neurons and thus, likely play a simple information integration role. Layer 5b neurons, in contrast, have larger cell bodies and exhibit “intrinsic bursting” properties at ~10 Hz when over threshold (Connors, Gutnick, & Prince, 1982; Silva, Amitai, & Connors, 1991; Franceschetti et al., 1995).

Thalamic neurons...

Layer 5b neurons project to Layer 6 whose neurons can also be roughly divided into corticocortical (CC) and corticothalamic (CT) subtypes (Thomson, 2010).

Both Layer 6 CC neurons have properties similar to Layer 5a neurons – they collect inputs from other Layer 6a neurons and pass it to Layer 6 CT neurons. Layer 6 CT neurons project specifically to the thalamus and also receive direct thalamic input forming a small circuit. They have

This rhythmic firing has been shown to persist even with constant sensory stimulation *in vivo* (Luczak, Bartho, & Harris, 2013), suggesting that Layer 5 neurons' alpha rhythmicity could

implement a roughly 10 Hz gating function for spikes relayed to Layer 6 neurons.

Thus, Layer 6 specifically becomes the neural substrate of the SRN's temporally lagged context representation, representing information that is, on average, one alpha cycle (approximately 100 ms) in the past. This contextual storage occurs at an automatic interval due to the intrinsic pacemaking properties of Layer 5 neurons, and might implement a reference frame that essentially would allow the brain to know *when* to anticipate inputs. As such, intrinsic oscillations have been shown to phase lock to environmental stimulation (Will & Berg, 2007; Lakatos, Karmos, Mehta, Ulbert, & Schroeder, 2008; Schroeder & Lakatos, 2009; Stefanics, Hangya, Herndi, Winkler, Lakatos, & Ulbert, 2010), ensuring environmental events coincide with key events like Layer 5 bursts in cortex.

Layer 6 sends axons toward the thalamus, completing the microcircuit within the local column and allowing the temporally lagged Layer 6 information to integrate with more current Layer 4 inputs. There also exists a direct connection between Layer 6 and Layer 4, that could be used for this purpose, although it has been noted as being weak compared to other intracolumnar connections (Hirsch & Martinez, 2006). In either case, temporal associations could be created by simple Hebbian learning mechanisms that track high probability co-occurrences across past and present events.

The Leabra algorithm (O'Reilly & Munakata, 2000; O'Reilly et al., 2012), however, also makes use of powerful error-driven learning (in addition to more standard Hebbian learning). In the context of temporal integration, error-driven learning would allow computation of error signals based on the difference between what is predicted to happen at a given moment (given the previous moments context as an input) and what actually happens. However, this computation requires that both the prediction and the actual sensation are represented subsequently within a single alpha cycle, which is not possible if the sensory periphery is always transmitting incoming inputs. To resolve this issue, the LeabraTI framework posits a mechanism to modulate or even block the transmission of inputs from the sensory periphery. A subset of cells in the thalamus exhibit alpha spectrum bursting properties similar to that of Layer 5 neurons (Lopes da Silva, 1991; Hughes

et al., 2004; Lorincz, Crunelli, & Hughes, 2008; Lorincz, Kekesi, Juhasz, Crunelli, & Hughes, 2009), and thus perhaps perform a similar gating function. Specifically, these neurons appear to shift the balance of inputs to Layer 4 and superficial neurons between exogenous environmental inputs and endogenous inputs local to the microcolumn.

When environmental inputs are downmodulated or blocked, Layer 6 context relayed via the thalamus is the dominant input to the microcolumn, which can be used to predict the incoming sensory event during the latter part of the alpha cycle. Importantly, during both the prediction and sensation phases, feedforward and feedback projections are constantly transmitting between lower and higher cortical areas. As previously mentioned, these projections originate and terminate predominantly in superficial layers, boosting their spike coherence to higher frequency spectra. This could potentially explain the differentially high gamma power in superficial layers compared to deep layers, and provides a compelling link between gamma oscillations and predicting specific details about the next sensory event.

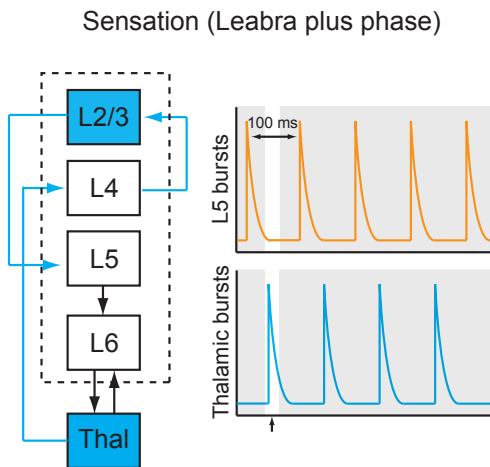
### **2.2.3 Summary of LeabraTI computation**

The overall computation of LeabraTI is shown in Figure 2.2 and summarized here. When thalamic cells burst (roughly every 100 ms), information from the sensory periphery is the primary driving force for Layer 4 neurons in primary cortex. This information is relayed downstream to higher-level cortical areas via the strong feedforward Layer 4 → Layer 2/3 → Layer 4 pathway (Felleman & Van Essen, 1991). Within the local microcolumn, Layer 5 neurons integrate this information, until thalamic bursting quiets (generally around 50 ms). At this point, Layer 5 cells burst, sending outputs to Layer 6 and shifting and inputs to the microcolumn endogenously. The information represented by Layer 6 neurons is temporally lagged (from the previous 50 ms) and is relayed to Layer 4 via non-bursting (regular spiking) thalamic neurons or via the direct Layer 6 → Layer 4 connection (not pictured in Figure 2.2), and might be maintained by reciprocal thalamo-cortical drive back to Layer 6. This information can be used as a prediction as to what will happen next when thalamic bursting resumes and veridical sensory information serves as the input once

again. In the context of Leabra's error-driven learning these two phases correspond to the plus phase (sensation) and minus phase (prediction), which can be used to compute a sensory prediction error signal. This error signal modifies Layer 5 → Layer 6 synapses to minimize differences between predictions and sensations over time.

Critically, for the LeabraTI computation to work, thalamic and Layer 5 oscillatory phases need to have an approximately antiphase relationship in order for the error-driven learning scheme described here to work so that Layer 2/3 neurons can represent the current moment's prediction with Layer 6 context as their primary input and then subsequently represent the veridical sensory input while Layer 5 neurons are queuing up the next contextual event. Such a relationship has not yet been shown yet, but very few studies have recorded simultaneously from thalamic and cortical neurons *in vivo* in the awake behaving animal. It is also possible that the brain implements error-driven learning in such a way that does not require representing predictions and sensations temporally interleaved on the same neural substrate or even that the brain accomplishes temporal integration completely without supervision, which in case thalamic gating is not required.

a)



b)

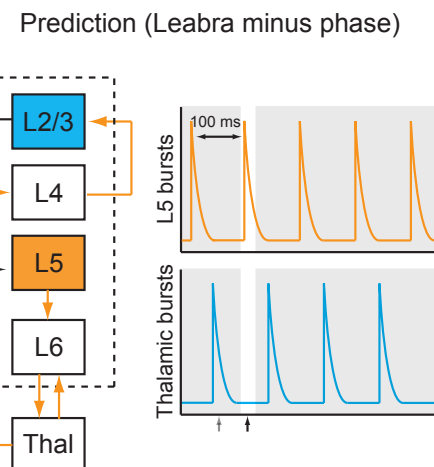


Figure 2.2: The LeabraTI model computation.

## 2.3 LeabraTI predictions

### 2.3.1 Relation to existing models

### 2.3.2 Testable predictions

**TODO**

## References

- Armstrong-James, M., Fox, K., & Das-Gupta, A. (1992). Flow of excitation within rat barrel cortex on striking a single vibrissa. *Journal of Neurophysiology*, *68*(4), 1345–1358.
- Arnal, L. H., & Giraud, A.-L. (2012). Cortical oscillations and sensory predictions. *Trends in Cognitive Sciences*, *16*(7), 390–398.
- Balas, B. J., & Sinha, P. (2009). The role of sequence order in determining view canonicality for novel wire-frame objects. *Attention, Perception & Psychophysics*, *71*(4), 712–723.
- Benjamini, Y., & Yekutieli, D. (2001). The control of the false discovery rate in multiple testing under dependency. *The Annals of Statistics*, *29*(4), 1165–1188.
- Brainard, D. (1997). The Psychophysics Toolbox. *Spatial Vision*, *10*(4), 433–436.
- Buffalo, E. A., Fries, P., Landman, R., Buschman, T. J., & Desimone, R. (2011). Laminar differences in gamma and alpha coherence in the ventral stream. *Proceedings of the National Academy of Sciences of the United States of America*, *108*(27), 11262–11267.
- Bulthoff, H. H., & Edelman, S. (1992). Psychophysical support for a two-dimensional view interpolation theory of object recognition. *Proceedings of the National Academy of Sciences of the United States of America*, *89*(1), 60–64.
- Busch, N. A., Dubois, J., & VanRullen, R. (2009). The phase of ongoing EEG oscillations predicts visual perception. *The Journal of Neuroscience*, *29*(24), 7869–7876.
- Buxhoeveden, D. P., & Casanova, M. F. (2002). The minicolumn hypothesis in neuroscience. *Brain*, *125*(Pt 5), 935–951.
- Connors, B. W., Gutnick, M. J., & Prince, D. A. (1982). Electrophysiological properties of neocortical neurons in vitro. *Journal of Neurophysiology*, *48*(6), 1302–1320.
- Cousineau, D. (2005). Confidence intervals in within-subject designs: A simpler solution to Loftus and Massons method. *Tutorials in Quantitative Methods for Psychology*, *1*(1), 42–45.
- Delorme, A., & Makeig, S. (2004). EEGLAB: An open source toolbox for analysis of single-trial EEG dynamics including independent component analysis. *Journal of Neuroscience Methods*, *134*(1), 9–21.
- Doherty, J. R., Rao, A., Mesulam, M. M., & Nobre, A. C. (2005). Synergistic effect of combined temporal and spatial expectations on visual attention. *The Journal of Neuroscience*, *25*(36), 8259–8266.
- Douglas, R. J., & Martin, K. A. C. (2004). Neuronal circuits of the neocortex. *Annual Review of Neuroscience*, *27*, 419–451.
- Edelman, S., & Bulthoff, H. H. (1992). Orientation dependence in the recognition of familiar and novel views of three-dimensional objects. *Vision Research*, *32*(12), 2385–2400.
- Elman, J. L. (1990). Finding structure in time. *Cognitive Science*, *14*(2), 179–211.
- Fahrenfort, J. J., Scholte, H. S., & Lamme, V. A. F. (2007). Masking disrupts reentrant processing in human visual cortex. *Journal of Cognitive Neuroscience*, *19*(9), 1488–1497.

- Felleman, D. J., & Van Essen, D. C. (1991). Distributed hierarchical processing in the primate cerebral cortex. *Cerebral Cortex*, *1*(1), 1–47.
- Foldiak, P. (1991). Learning invariance from transformation sequences. *Neural Computation*, *3*(2), 194–200.
- Franceschetti, S., Guatteo, E., Panzica, F., Sancini, G., Wanke, E., & Avanzini, G. (1995). Ionic mechanisms underlying burst firing in pyramidal neurons: Intracellular study in rat sensorimotor cortex. *Brain Research*, *696*(1–2), 127–139.
- Giraud, A.-L., & Poeppel, D. (2012). Cortical oscillations and speech processing: Emerging computational principles and operations. *Nature Neuroscience*, *15*(4), 511–517.
- Hirsch, J. A., & Martinez, L. M. (2006). Laminar processing in the visual cortical column. *Current Opinion in Neurobiology*, *16*(4), 377–384.
- Horton, J. C., & Adams, D. L. (2005). The cortical column: A structure without a function. *Philosophical Transactions of the Royal Society B*, *360*(1456), 837–862.
- Hubel, D. H., & Wiesel, T. N. (1977). Ferrier lecture. Functional architecture of macaque monkey visual cortex. *Proceedings of the Royal Society B*, *198*(1130), 1–59.
- Hughes, S. W., Lorincz, M., Cope, D. W., Blethyn, K. L., Kekesi, K. A., Parri, H. R., Juhasz, G., & Crunelli, V. (2004). Synchronized oscillations at alpha and theta frequencies in the lateral geniculate nucleus. *Neuron*, *42*(2), 253–268.
- Jones, E. G. (2000). Microcolumns in the cerebral cortex. *Proceedings of the National Academy of Sciences of the United States of America*, *97*(10), 5019–5021.
- Lachaux, J. P., Rodriguez, E., Martinerie, J., & Varela, F. J. (1999). Measuring phase synchrony in brain signals. *Human Brain Mapping*, *8*(4), 194–208.
- Lakatos, P., Karmos, G., Mehta, A. D., Ulbert, I., & Schroeder, C. E. (2008). Entrainment of neuronal oscillations as a mechanism of attentional selection. *Science*, *320*(5872), 110–113.
- Logothetis, N., Pauls, J., Bulthoff, H., & Poggio, T. (1994). View-dependent object recognition by monkeys. *Current Biology*, *4*(5), 401–414.
- Logothetis, N. K., Pauls, J., & Poggio, T. (1995). Shape representation in the inferior temporal cortex of monkeys. *Current Biology*, *5*(5), 552–563.
- Lopes da Silva, F. (1991). Neural mechanisms underlying brain waves: from neural membranes to networks. *Electroencephalography and Clinical Neurophysiology*, *79*(2), 81–93.
- Lorincz, M. L., Crunelli, V., & Hughes, S. W. (2008). Cellular dynamics of cholinergically induced alpha (8–13 Hz) rhythms in sensory thalamic nuclei in vitro. *The Journal of Neuroscience*, *28*(3), 660–671.
- Lorincz, M. L., Kekesi, K. A., Juhasz, G., Crunelli, V., & Hughes, S. W. (2009). Temporal framing of thalamic relay-mode firing by phasic inhibition during the alpha rhythm. *Neuron*, *63*(5), 683–696.
- Luczak, A., Bartho, P., & Harris, K. D. (2013). Gating of sensory input by spontaneous cortical activity. *The Journal of Neuroscience*, *33*(4), 1684–1695.

- Lumer, E., Edelman, G., & Tononi, G. (1997). Neural dynamics in a model of the thalamocortical system. I. Layers, loops and the emergence of fast synchronous rhythms. *Cerebral Cortex*, *7*(3), 207–227.
- Masquelier, T., & Thorpe, S. J. (2007). Unsupervised learning of visual features through spike timing dependent plasticity. *PLoS Computational Biology*, *3*(2), 247–257.
- Mathewson, K. E., Lleras, A., Beck, D. M., Fabiani, M., Ro, T., & Gratton, G. (2011). Pulsed out of awareness: EEG alpha oscillations represent a pulsed-inhibition of ongoing cortical processing. *Frontiers in Psychology*, *2*.
- Mountcastle, V. B. (1997). The columnar organization of the neocortex. *Brain*, *120*(Pt 4), 701–722.
- Mutch, J., & Lowe, D. (2008). Object class recognition and localization using sparse features with limited receptive fields. *International Journal of Computer Vision*, *80*(1), 45–57.
- Oostenveld, R., Fries, P., Maris, E., & Schoffelen, J.-M. (2011). FieldTrip: Open source software for advanced analysis of MEG, EEG, and invasive electrophysiological data. *Computational Intelligence and Neuroscience*, *2011*.
- O'Reilly, R. C., & Munakata, Y. (2000). *Computational Explorations in Cognitive Neuroscience: Understanding the Mind by Simulating the Brain*. Cambridge, MA: The MIT Press.
- O'Reilly, R. C., Munakata, Y., Frank, M. J., Hazy, T. E., & Contributors (2012). *Computational Cognitive Neuroscience*. Wiki Book, 1st Edition, URL: <http://ccnbook.colorado.edu>.
- Pelli, D. (1997). The VideoToolbox software for visual psychophysics: Transforming numbers into movies. *Spatial Vision*, *10*(4), 437–442.
- Perrin, F., Pernier, J., Bertrand, O., & Echallier, J. F. (1989). Spherical splines for scalp potential and current density mapping. *Electroencephalography and Clinical Neurophysiology*, *72*(2), 184–187.
- Rockland, K. S., & Pandya, D. N. (1979). Laminar origins and terminations of cortical connections of the occipital lobe in the rhesus monkey. *Brain Research*, *179*(1), 3–20.
- Rohenkohl, G., & Nobre, A. C. (2011). Alpha oscillations related to anticipatory attention follow temporal expectations. *The Journal of Neuroscience*, *31*(40), 14076–14084.
- Schroeder, C. E., & Lakatos, P. (2009). Low-frequency neuronal oscillations as instruments of sensory selection. *Trends in Neurosciences*, *32*(1), 9–18.
- Serre, T., Oliva, A., & Poggio, T. (2007). A feedforward architecture accounts for rapid categorization. *Proceedings of the National Academy of Sciences of the United States of America*, *104*(15), 6424–6429.
- Servan-Schreiber, D., Cleeremans, A., & McClelland, J. L. (1991). Graded state machines: The representation of temporal contingencies in simple recurrent networks. *Machine Learning*, *7*(2–3), 161–193.
- Silva, L. R., Amitai, Y., & Connors, B. W. (1991). Intrinsic oscillations of neocortex generated by layer 5 pyramidal neurons. *Science*, *251*(4992), 432–435.

- Sinha, P., & Poggio, T. (1996). Role of learning in three-dimensional form perception. *Nature*, 384(6608), 460–463.
- Spaak, E., Bonnefond, M., Maier, A., Leopold, D. A., & Jensen, O. (2012). Layer-specific entrainment of gamma-band neural activity by the alpha rhythm in monkey visual cortex. *Current Biology*, 22(24), 2313–2318.
- Stefanics, G., Hangya, B., Herndi, I., Winkler, I., Lakatos, P., & Ulbert, I. (2010). Phase entrainment of human delta oscillations can mediate the effects of expectation on reaction speed. *The Journal of Neuroscience*, 30(41), 13578–13585.
- Thomson, A. M. (2010). Neocortical layer 6, a review. *Frontiers in Neuroanatomy*, 4.
- Thomson, A. M., & Lamy, C. (2007). Functional maps of neocortical local circuitry. *Frontiers in Neuroscience*, 1(1), 19–42.
- Townshend, J. T., & Ashby, F. G. (1983). *Stochastic Modeling of Elementary Psychological Processes*. Cambridge: Cambridge University Press.
- Townshend, J. T., & Ashby, F. G. (2005). Methods of modeling capacity in simple processing systems. In J. N. Castellan Jr., & F. Restle (Eds.), *Cognitive Theory: Volume 3* (pp. 200–239). Hillsdale, NJ: Lawrence Erlbaum Associates.
- VanRullen, R., Busch, N. A., Drewes, J., & Dubois, J. (2011). Ongoing EEG phase as a trial-by-trial predictor of perceptual and attentional variability. *Frontiers in Psychology*, 2.
- Will, U., & Berg, E. (2007). Brain wave synchronization and entrainment to periodic acoustic stimuli. *Neuroscience letters*, 424(1), 55–60.

## **Chapter 3**

### **Spatial and temporal prediction during novel object recognition: Temporal and spectral signatures**

#### **3.1 Introduction**

TODO, pull from proposal and proposal-r1. Try to write without referencing LeabraTI too much, this chapter should stand by itself

#### **3.2 Methods**

##### **3.2.1 Participants**

A total of 58 students from the University of Colorado Boulder participated in the experiment (ages 18-28 years, mean=21; 31 male, 27 female). EEG was recorded from 29 of the participants while they completed the experiment. The remaining 29 participants completed a solely behavioral experiment without EEG recording. All participants were right-handed and reported normal or corrected-to-normal vision. Participants either received course credit or payment of \$15 per hour as compensation for their participation. Informed consent was obtained from each participant prior to the experiment in accordance with Institutional Review Board policy at the University of Colorado.

##### **3.2.2 Stimuli**

Novel “paper clip” objects similar to those used in previous studies (Bulthoff & Edelman, 1992; Edelman & Bulthoff, 1992; Logothetis, Pauls, Bulthoff, & Poggio, 1994; Logothetis, Pauls, &

Poggio, 1995; Sinha & Poggio, 1996) were created using MATLAB. Eight vertices were placed randomly on the surface of a sphere of unit radius and then joined together with line segments. The last and first vertex were also joined to form a closed loop so that line segment terminations were not a salient feature (Balas & Sinha, 2009). Objects were constrained to exclude extremely acute angles between successive segments (less than 20 degrees) and were approximately rotationally balanced (center of mass within 10% of the origin). Objects were rotated completely about their vertical axis in steps of 12 degrees and rendered to bitmap images under an orthographic projection. A total of 16 objects were created using this procedure, yielding 480 images (30 images per object). Object examples are shown in Figure 3.1.

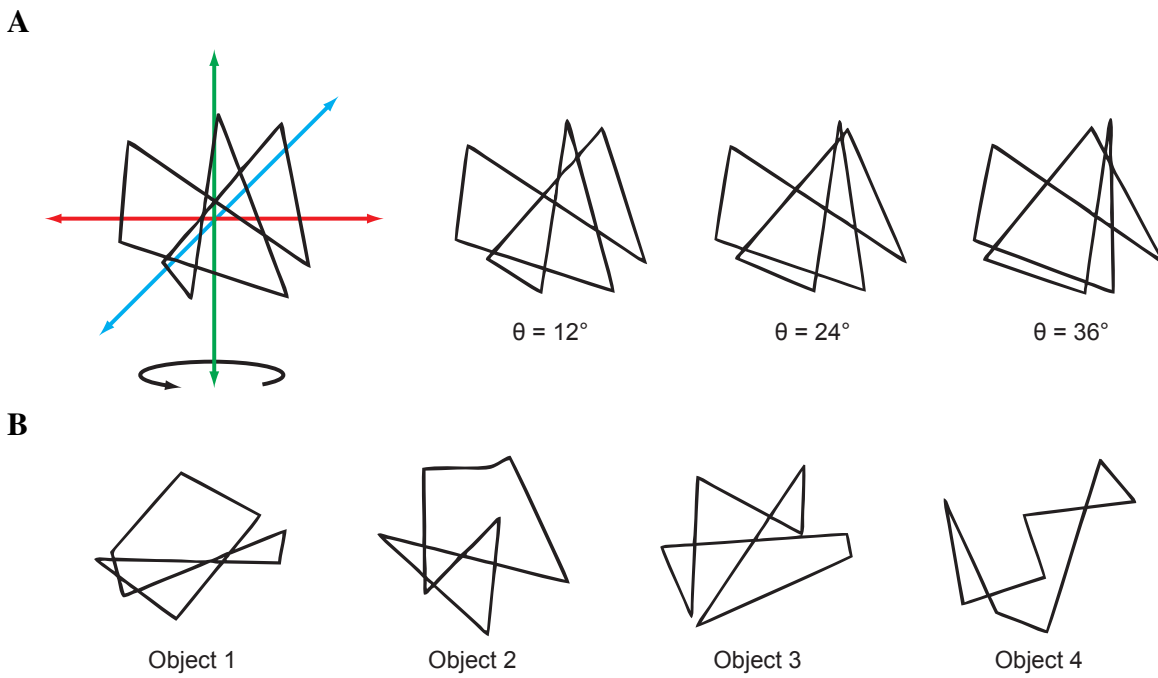


Figure 3.1: Novel “paper clip” objects

**A:** Objects were composed of eight three-dimensional vertices joined together with line segments. To render the objects to bitmap images, each object was rotated completely about its vertical axis in steps of 12 degrees and reduced to an orthographic projection. **B:** Four of the 16 objects used in the experiment.

### 3.2.3 Procedure

Participants observed an entraining sequence of rotated views of a random object and performed a same-different judgement about a probe stimulus. On each trial, a view was randomly selected as the initial view of the sequence followed by seven additional views spaced 24 degrees apart (Figure 3.2A, blue tick marks). Thus, the eight view entraining sequence spanned 168 degrees of the object. The entraining sequence was either presented in order (i.e., spatially predictable) or randomized. Following the entraining sequence after a 200 ms blank was a probe stimulus consisting of either an unseen view from the entraining object or a novel distractor. Unseen views were randomly sampled from the 12 degree interpolations between views of the entraining sequence (Figure 3.2A, magenta tick marks) and from outside of the span of the entraining sequence in increments of 24 degrees (Figure 3.2A, green tick marks).

Distractors were created from the original target objects by randomly selecting new spherical coordinates for six of the eight vertices and re-rendering them to bitmap images using the same method as the original target objects (12 degree steps about the vertical axis). Distractors conformed to the same constraints as the original target objects (no extremely acute angles, approximately rotationally balanced). Participants were instructed to respond “same” if they believed the probe depicted the same object as the entraining sequence or “different” if it depicted a distractor object. Participants received feedback after each trial according to whether their response was correct or incorrect.

During the entraining sequence, object views were presented for 50 ms at either 10 Hz (i.e., temporally predictable) or at a variable rate by manipulating the interstimulus interval (ISI) between subsequent views. Temporally predictable ISIs were 50 ms, totaling 350 ms across the entraining sequence. Variable ISIs were selected by randomly generating seven ISIs that also summed to 350 ms (Figure 3.2B). ISIs were in the range of 16.67 ms (minimum) to 216.67 ms (maximum) in increments of 16.67 ms. Temporal unpredictability was maximized by generating 400 such ISI sequences, calculating the summed squared error (SSE) across subsequent ISIs in a

sequence, and selecting the 100 sequences with the highest SSE for use during the experiment.

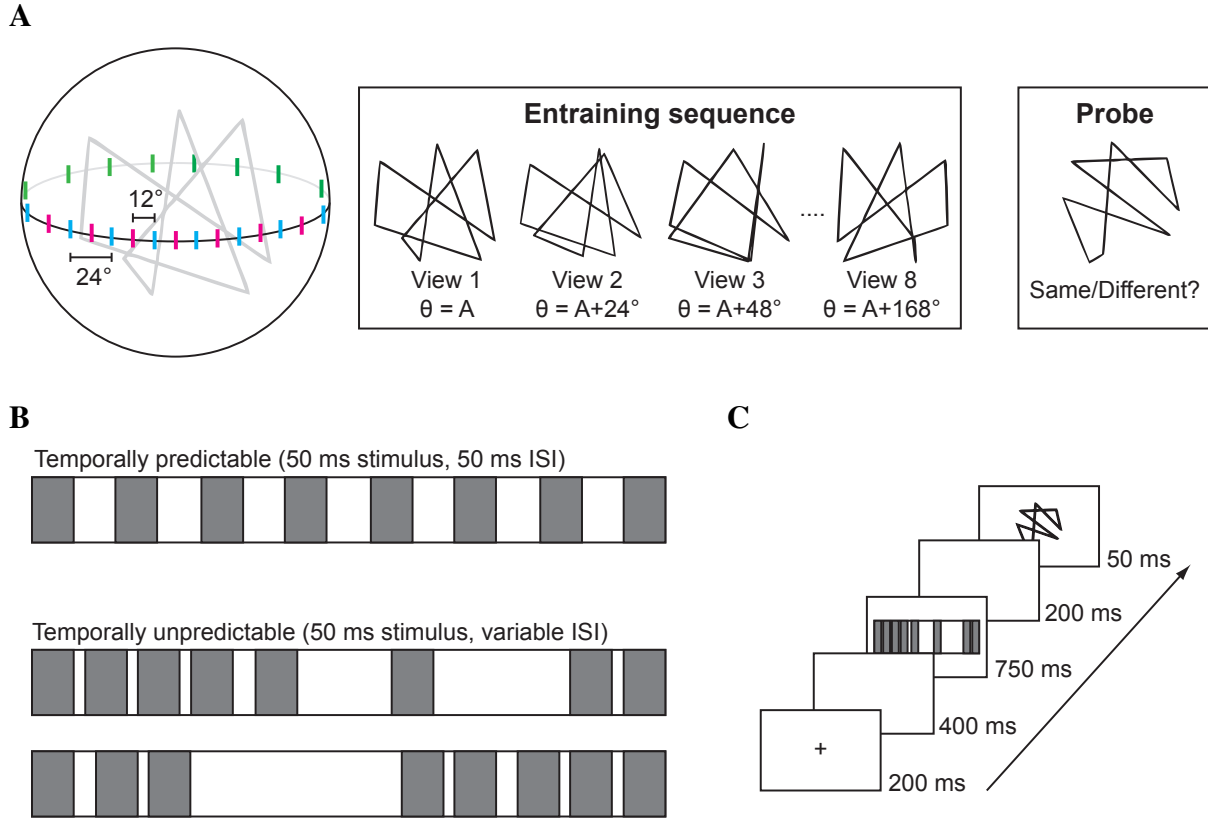


Figure 3.2: Experimental procedure

**A:** Experimental trials contained an entraining sequence composed of eight views of a single object, followed by a probe stimulus. Entrainning views were spaced 24 degrees apart (blue tick marks). The probe depicted an unseen view from the 12 degree interpolations between views of the entraining sequence (magenta tick marks) or from outside the span of the entraining sequence in increments of 24 degrees (green tick marks). **B:** Entrainning views were either presented at 10 Hz with a 50 ms on time and 50 ms off time or in a temporally unpredictable manner with a 50 ms on time (gray segments) and variable off time (white segments). In both cases, the duration of the total entraining sequence was held constant at 750 ms. **C:** Order and timing of events within a single trial.

The experiment was displayed on an LCD monitor at native resolution operating at 60 Hz using the Psychophysics Toolbox Version 3 (Brainard, 1997; Pelli, 1997). Stimuli were presented on an isoluminant 50% gray background and subtended approximately 5 degrees of visual angle. Trials began with a fixation cross (200 ms) followed by a blank (400 ms), the entraining sequence

(750 ms total), a second blank (200 ms), and ended with the probe stimulus (50 ms) (Figure 3.2C). Participants were required to respond within 2000 ms. Trials were separated by a variable intertrial interval of 2000-2400 ms. The experiment contained 500 trials with an additional 20 practice trials that contained a longer blank (1000 ms) between the entraining sequence and the probe to familiarize participants with the order of events during trials. Participants completed the 20 practice trials (which were discarded from analysis) prior to performing the 500 experimental trials.

### **3.2.4 EEG recording and preprocessing**

The EEG was recorded using an Electrical Geodesics, Inc. (EGI) system composed of a 128 channel net (HCGSN 130) amplified through  $200\text{ M}\Omega$  amplifiers (Net Amps 200). The signal was sampled at 250 Hz with impedances for each electrode were adjusted to less than  $40\text{ k}\Omega$  before and during the recording. Stimulus and response trigger onsets were measured via the Psychophysics Toolbox using a high precision realtime clock that was synchronized within 2.5 ms of the EEG system's clock before every trial during the experiment.

EEG data were preprocessed using the FieldTrip toolbox (Oostenveld, Fries, Maris, & Schoffelen, 2011). Raw data were first band-pass filtered between 1 Hz and 100 Hz with a 59-61 Hz band-stop and then epoched into 2350 ms segments that spanned the start of the pre-trial blank to 1000 ms after the probe stimulus. Individual segments were visually inspected and rejected if found to contain muscle artifacts or atypical noise. Bad channels were also identified and temporarily removed from the data before performing ICA decomposition (Delorme & Makeig, 2004) to remove of ocular artifacts. Components related to ocular artifacts were identified based on their topographical distribution across electrodes. The data were reconstructed without the ocular components and any bad channels were replaced using spherical spline interpolation (Perrin, Pernier, Bertrand, & Echallier, 1989). The resulting segments were re-referenced to the average reference.

### 3.2.5 Event-related averaging

Event-related averaging was performed separately for the entraining sequence and the subsequent probe. For the entraining sequence, data were aligned to the onset of entraining views 2 through 8 and averaged from the period beginning 50 ms before each entrainer and ending 50 ms after. Baseline correction was performed using the first 50 ms of this period. For the probe, data were aligned to the probe onset and averaged from the period beginning 200 ms before the probe and ending 400 ms after. This allowed detection of predictability effects during the blank period due to differences in phase elicited by the entraining sequence as well as probe-evoked predictability effects.

All waveforms were averaged over a montage of 23 electrodes that covered the occipital and parietal cortices (Figure 3.3). The montage included locations from the 10-10 system that are commonly associated with perceptual processing (Oz, O1/O2, PO3/PO4, and PO7/PO8) (e.g., Doherty, Rao, Mesulam, & Nobre, 2005; Rohenkohl & Nobre, 2011; Fahrenfort, Scholte, & Lamme, 2007).

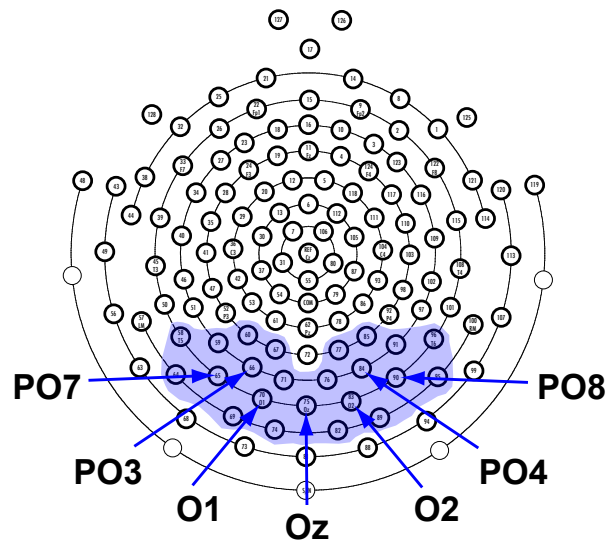


Figure 3.3: Electrode pooling for analyses

Blue shaded region denotes pooled electrodes. Locations from the 10-10 system are indicated.

### 3.2.6 Time-frequency analysis

Segmented data were used to compute time-frequency data for each trial. Data were first downsampled to 125 Hz and then used to compute the instantaneous Fourier coefficients at each time bin using a multi-taper approach. Hanning tapers were generated at 5-40 Hz and convolved with the data using a sliding time window (four cycles per frequency per time window). The relatively long time window required for low-frequency bands prevents computation of time-frequency data for short time segments, such as the 200 ms blank before the probe. To address this issue, time-frequency data was computed over the entire 2350 ms trial epoch and then cropped to investigate temporal regions of interest.

Power was computed from the magnitude of the instantaneous Fourier coefficients at each frequency ( $f$ ) and time bin ( $t$ ):

$$\text{Power}(f, t) = \frac{1}{n} \sum_{k=1}^n |F_k(f, t)|^2$$

Phase, which is normally defined as the angle of the complex Fourier coefficients, cannot be averaged due to its circularity and thus standard statistical models cannot be applied to assess its significance. One solution to this problem is to compute inter-trial coherence (ITC) instead (Lachaux, Rodriguez, Martinerie, & Varela, 1999). ITC is averaged in the complex domain by first normalizing phase information to unit length by dividing off power and computing the magnitude:

$$\text{ITC}(f, t) = \left| \frac{1}{n} \sum_{k=1}^n \frac{F_k(f, t)}{|F_k(f, t)|} \right|$$

ITC ranges between 0 and 1 and represents how systematic phase angles are across trials. A value of 0 indicates that phase information is essentially uniformly distributed across trials while a value of 1 indicates a high degree of phase-locking at a particular frequency across trials.

All time-frequency analyses were averaged over the same montage of 23 occipitoparietal electrodes that was used to compute event-related averages (Figure 3.3).

### 3.3 Results

#### 3.3.1 Behavioral measures of spatial and temporal predictability

Five subjects were excluded from behavioral analysis for accuracy  $2.7\sigma$  (or further) below mean accuracy across subjects. The remaining 53 subjects were submitted to a 2x2 ANOVA with spatial and temporal predictability as within-subjects factors. Experiment type (EEG or behavioral only) was included as an additional between-subjects factor to ensure that it did not interact with any of the within-subjects factors. Accuracy and reaction times were collected during the experiment and were used to compute  $d'$ , a measure of sensitivity that takes into account response bias, and inverse efficiency, a measure that combines accuracy and reaction times (Townshend & Ashby, 2005). These behavioral measures are plotted in Figure 3.4.

Subjects that completed the full EEG experiment were on average less accurate ( $F(1, 51) = 4.80, p = 0.033$ ) but responded more quickly ( $F(1, 51) = 10.05, p = 0.003$ ) than subjects that completed the solely behavioral experiment. These differences reflect a speed-accuracy tradeoff, likely due to differences in instructions given to subjects by experimenters or motivational differences between subject groups. Importantly, experiment type did not interact with any within-subjects factors (all  $p$ 's  $> 0.05$ ) indicating that the behavioral measures of interest were not dependent on which type of experiment subjects completed.

Overall, subjects were more accurate when the entraining sequence was temporally predictable ( $F(1, 51) = 17.84, p < 0.001$ ). A similar effect for spatial predictability failed to reach significance ( $F(1, 51) = 1.85, p = 0.18$ ). The interaction between spatial and temporal predictability, however, was significant ( $F(1, 51) = 6.13, p = 0.017$ ). The LeabraTI model (Chapter 2) as well as previous investigations of predictability (e.g., Doherty et al., 2005) suggest that spatial and temporal predictability should have an additive effect on behavioral outcomes. However, the combined spatial and temporal predictability condition here (denoted S+T+ in Figure 3.4) is sub additive. Although not significantly different from spatial predictability alone ( $t(52) = 1.29, p = 0.204$ ) or from temporal predictability alone ( $t(52) = 0.45, p = 0.652$ ), this result merits further

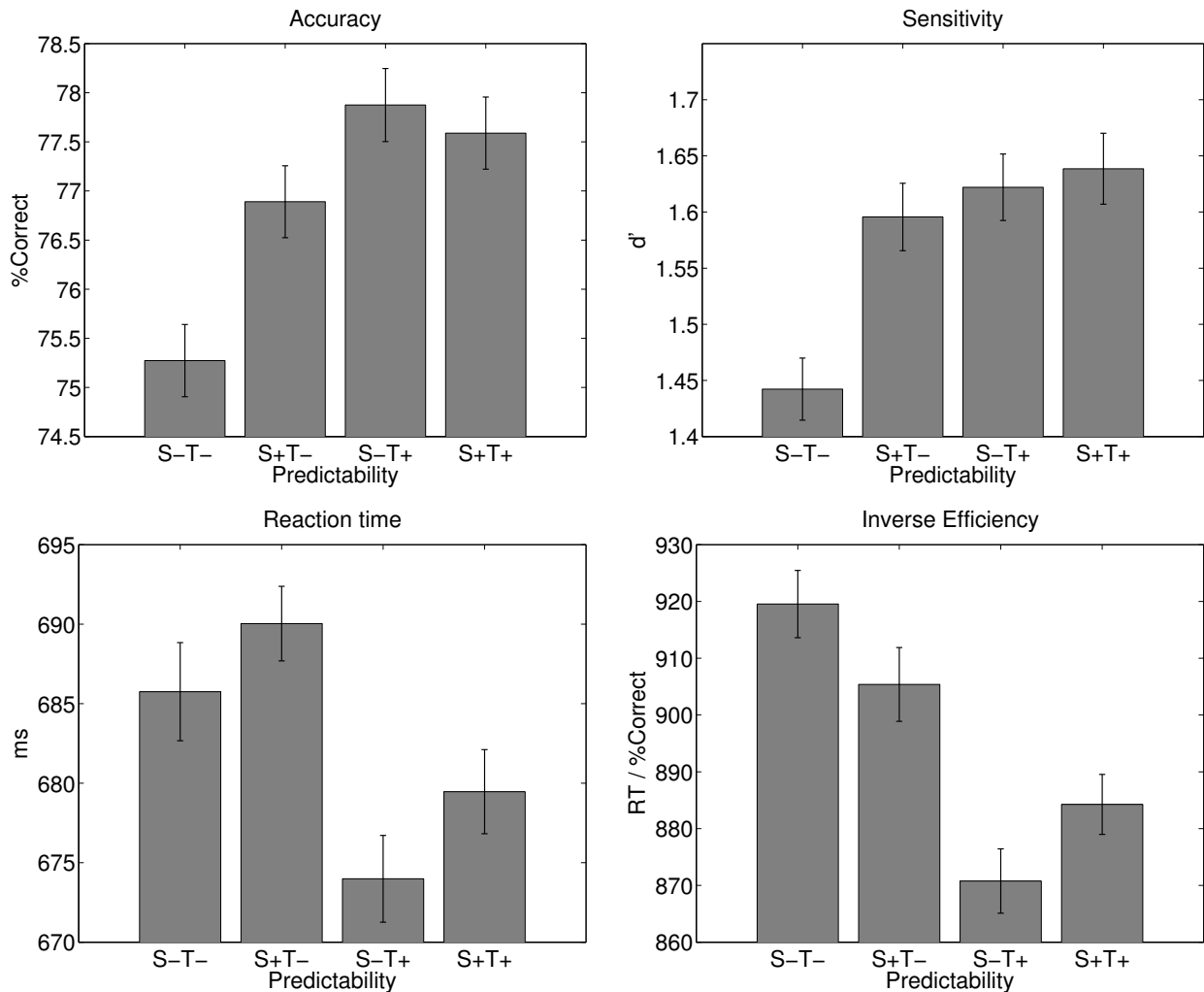


Figure 3.4: Behavioral measures of spatial and temporal predictability

Accuracy,  $d'$  (sensitivity), reaction time, and inverse efficiency (reaction time divided by percent correct) as a function of entrainment condition. S-/+ refers to spatially unpredictable and predictable, T-/+ to temporally unpredictable and predictable. Error bars depict within-subjects error using the method described in Cousineau (2005) adapted for standard error.

investigation.

When responses are transformed into  $d'$ , there is a significant effect of both spatial ( $F(1, 51) = 4.71, p = 0.035$ ) and temporal predictability ( $F(1, 51) = 11.99, p < 0.001$ ). This result suggests that response bias can at least partially explain why spatial predictability failed to reach significance for raw accuracy. The interaction between spatial and temporal predictability remained significant

for  $d'$  ( $F(1, 51) = 4.49, p = 0.039$ ). The interaction is additive, but is driven primarily by the strong effect of introducing spatial or temporal predictability over complete unpredictability (S-T- versus S+T-,  $t(52) = 3.19, p = 0.002$ ; S-T- versus S+T+,  $t(52) = 4.26, p < 0.001$ ) opposed to any synergistic effect of combined spatial and temporal predictability (S+T+ versus S+T-,  $t(52) = 0.90$ ; S+T+ versus S-T+,  $t(52) = 0.31$ ; both  $p$ 's  $> 0.05$ ).

Reaction times were significantly faster when the entraining sequence was temporally predictable ( $F(1, 51) = 12.38, p < 0.001$ ). A similar effect for spatial predictability failed to reach significance ( $F(1, 51) = 1.96, p = 0.168$ ) nor did the interaction term ( $F(1, 51) = 0.05, p = 0.83$ ).

Inverse efficiency, which considers reaction time as a function of accuracy (defined as reaction time divided by percent correct) can be thought of as the amount of energy consumed by the system to produce a behavioral outcome (Townshend & Ashby, 1983). It is often used to remove non-monotonicities present in accuracy or reaction times alone, although that effect is not observed here. Nevertheless, it provides another lens under which to interpret the results, and thus it is considered here. Inverse efficiency was significantly lower when the entraining sequence was temporally predictable ( $F(1, 51) = 23.31, p < 0.001$ ), but not when it was spatially predictable ( $F(1, 51) = 0.002, p = 0.963$ ). Inverse efficiency is characterized by a significant cross-over interaction ( $F(1, 51) = 5.85, p = 0.019$ ). Spatial predictability of the entraining sequence produces lowers inverse efficiency over complete unpredictability. Inverse efficiency is lowest on average when stimuli are temporally predictable, but the addition of spatial predictability causes an increase in inverse efficiency.

### **3.3.2 Time course of spatial and temporal predictability**

A total of five subjects were excluded from EEG analysis – three for an overabundance of artifacts in the EEG recording resulting in low trial counts after rejection and two for accuracy  $2.7\sigma$  (or further) below mean accuracy across subjects (these two subjects were also excluded from behavioral analyses, see preceding section). The remaining 24 subjects were included in all EEG analyses.

A 2x2 ANOVA with spatial and temporal predictability as within-subjects factors was used to assess statistical significance at each time bin of event-related averages. *p*-values were corrected for a maximum false discovery rate (FDR) of 5% using the method described in Benjamini and Yekutieli (2001). Additionally, effects were only considered significant if they persisted for at least 16 ms.

To investigate the build-up of spatial and temporal predictability over the entraining sequence, activity from the second through final entraining views was averaged for each condition (the first entraining view is unpredictable, so it is omitted from the average). The results of this analysis are plotted in Figure 3.5. The first thing worth noting is that a large 10 Hz periodicity is present for the temporally predictable conditions (S-T+ and S+T+), phase-aligned approximately to the onset of each entrainer. Temporally unpredictable entrainers (S-T- and S+T-) are also approximately periodic. The reason for the 10 Hz periodicity in these conditions despite being temporally unpredictable is likely due to the 750 ms constant duration of the entraining sequence regardless of condition (Figure 3.2B). Presenting eight stimuli in 750 ms with a variable ISI is a 10 Hz presentation rate on average. Still, the temporally unpredictable entrainers exhibit markedly weaker amplitude and are approximately 180 degrees out of phase with the temporally predictable entrainers.

The effect of spatial predictability manifested 26 ms after the onset of the entrainer and persisted for at least another 24 ms (one quarter of the 10 Hz period). Temporal predictability, in contrast, manifested prior to (-38 through -22 ms pre-stimulus) and at the onset of the entrainer (-6 ms pre-stimulus through 18 ms post-stimulus). The effect of temporal predictability appears to be driven by the antiphase relationship between T- and T+ conditions at these time points. Together, these effects demonstrate differential time courses for spatial and temporal predictability.

Spatial predictability was enhanced when stimuli were temporally predictable. This effect is characterized by the significant interaction between spatial and temporal predictability starting 14 ms after the onset of the entrainer and persisting for at least another 36 ms. This result indicates that the brain is more capable of differentiating between spatially coherent and random sequences

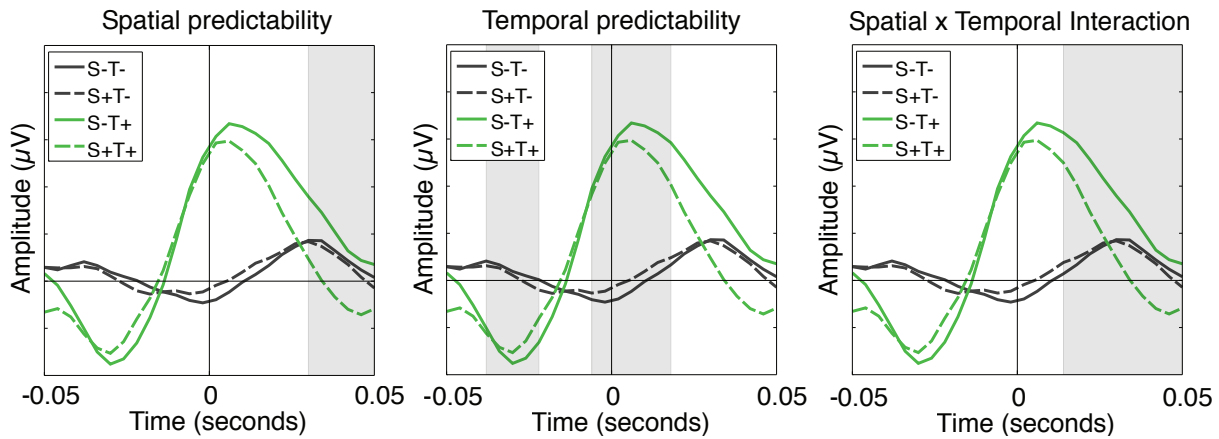


Figure 3.5: Entrainor-evoked activity

Grand averages for entrainers 2 through 8 as a function of entrainment condition. S-/+ refers to spatially unpredictable and predictable, T-/+ to temporally unpredictable and predictable. All plots depict the grand average with gray shaded regions denoting significant effects of spatial predictability (left), temporal predictability (center), and the interaction between these terms controlling for a maximum false discovery rate (FDR) of 5%.

of stimuli when it can properly anticipate the presentation of each stimulus (S-T+ versus S+T+) compared to when the onset is unpredictable.

To investigate the effect of spatial and temporal predictability on perception of the probe, waveforms were aligned to the probe onset onset averaged from 200 ms before through 400 ms after (Figure 3.6). The results of this analysis essentially mirror the entrainer-evoked effects albeit with a few key differences. Temporal predictability was again a purely anticipatory process, manifesting within the pre-stimulus period (-184 ms through -160 ms and -132 ms through -108 ms pre-stimulus). Spatial predictability also manifested briefly within the pre-stimulus period (-128 ms through -80 ms pre-stimulus), which was not seen for spatially predictable entrainers. The post-stimulus effects of spatial predictability occurred much earlier than for entrainers and persisted much longer, beginning approximately at the onset of the probe (-12 ms pre-stimulus) and lasting 136 ms through the P1 response with several transient effects after.

Unlike the significant interaction between spatial and temporal predictability for entrainers, the interaction for the probe failed to reach significance given the constraints of the statistical test

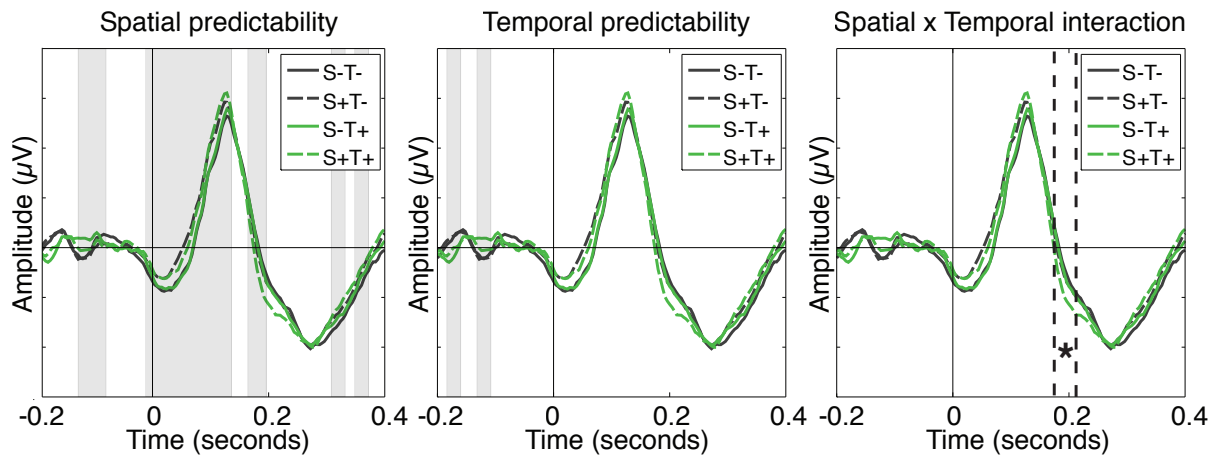


Figure 3.6: Probe-evoked activity

Grand averages for the probe stimulus, including the preceding 200 ms blank. Asterisk in the interaction plot indicates trending significance at the 5% level when averaging amplitude within the window defined by the dotted lines.

(maximum FDR of 5%, 16 ms consecutive significance). However, averaging the amplitude within a window defined by exploratory analysis indicated a trending interaction from 170 ms to 210 ms ( $F(1, 22) = 3.97, p = 0.059$ ). This effect was more pronounced and reached significance if only the right hemisphere channels were considered ( $F(1, 22) = 5.61, p = 0.027$ ), but failed to reach significance in the left hemisphere ( $F(1, 22) = 2.24, p = 0.148$ ), explaining the trending effect when both hemispheres are considered jointly.

### 3.3.3 Predictability entrains alpha oscillations

The same 24 subjects used in event-related analyses (see preceding section) were used in time-frequency analyses described here. Statistical methods were also identical, consisting of a 2x2 ANOVA with spatial and temporal predictability as within-subjects factors and  $p$ -values were corrected for a 5% maximum FDR (Benjamini & Yekutieli, 2001). Effects were only considered significant if they persisted for at least 16 ms.

Power and inter-trial coherence (ITC), a measure of phase angle consistency across trials (Lachaux et al., 1999) were computed over a 5-20 Hz frequency range to investigate the rela-

tionship between entrainer predictability and alpha oscillatory properties (Figures 3.7-3.8). Both spatial and temporal predictability had a significant effect on 10 Hz power and ITC beginning around 200 ms after the onset of the first entrainer (power: 160-168 ms after entrainer 1; ITC: 136-208 ms after entrainer 1). Together, these results indicate that 10 Hz entrainment affects both power and phase alignment and takes around 2-3 events to establish. Spatial predictability had a suppressive effect on 10 Hz power and phase alignment whereas temporal predictability had a positive effect. Any interactions between spatial and temporal predictability failed to reach significant levels altogether.

The effect of spatial predictability only persisted for three entrainers on average (duration ranges for 10 Hz power and ITC: 272-280 ms). Temporal predictability, in contrast, exhibited a sustained effect on 10 Hz power lasting nearly the entire entraining sequence. In the case of ITC, the effect of temporal predictability persisted throughout the blank period that separated the entraining sequence and the probe (Figure 3.9). This result indicates that alpha phase remained more aligned for temporally predictable stimuli even without exogenous entrainment.

Predictability effects on 10 Hz ITC failed to reach significance during the presentation of the probe or the following 400 ms period given the constraints of the statistical test (maximum FDR of 5%, 16 ms consecutive significance). An enhancement in ITC could be observed for the combined predictability (S+T+) condition and trended toward significance when averaged over a 100 ms period beginning 155 ms after the onset of the probe ( $F(1, 22) = 4.11, p = 0.055$ ). This effect was more pronounced and reached significance if only the right hemisphere channels were considered ( $F(1, 22) = 7.45, p = 0.012$ ), but failed to reach significance in the left hemisphere ( $F(1, 22) = 1.47, p = 0.237$ ), explaining the trending effect when both hemispheres are considered jointly.

### **3.3.4 Predictability effects in delta-theta bands**

The effects of spatial and temporal predictability on oscillatory properties during the probe period (-200 ms pre-stimulus through 400 ms after) were investigated in the delta-theta bands,

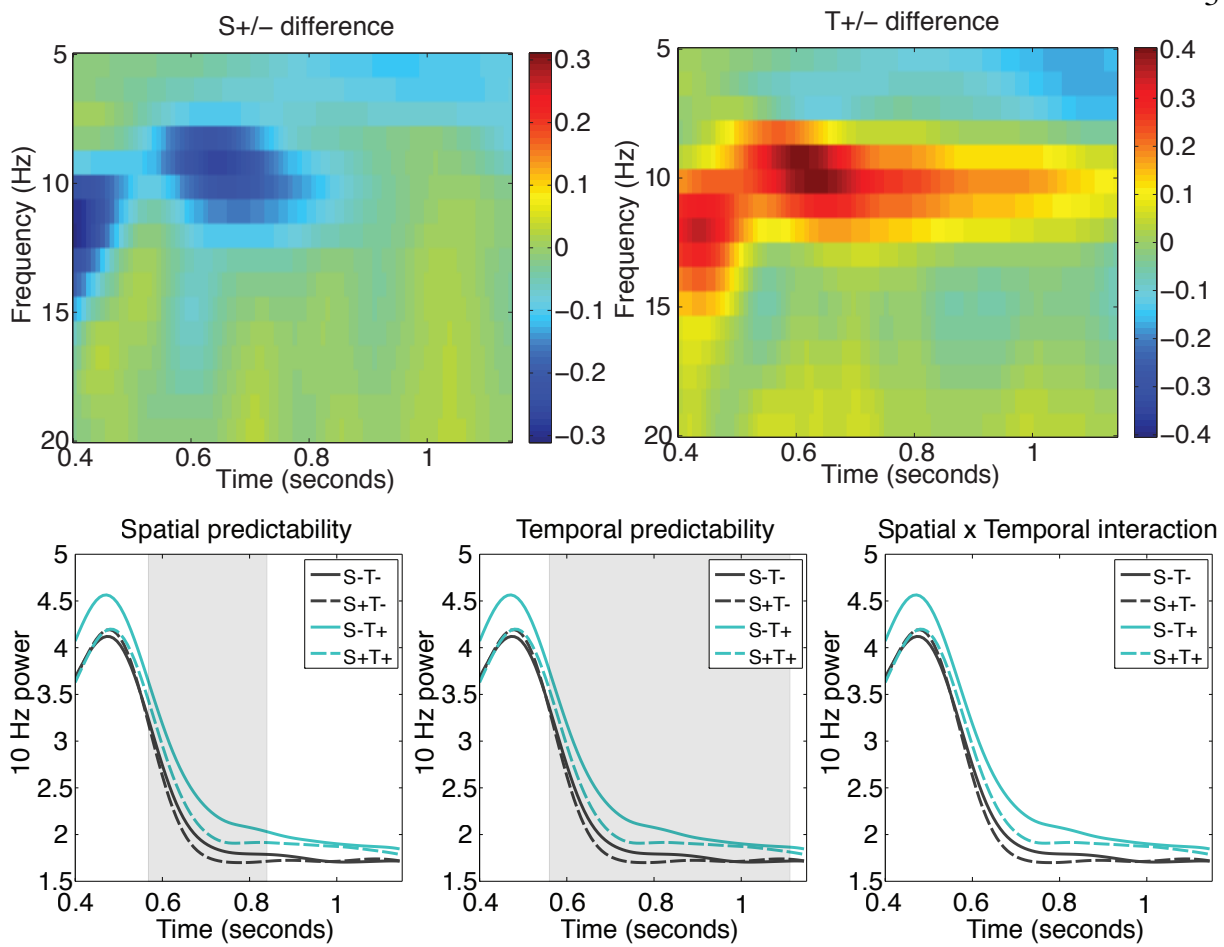


Figure 3.7: Effect of entrainer predictability on alpha power

Alpha-band power over the entraining sequence. **Top:** Main effects of spatial and temporal predictability on oscillatory power in the 5-20 Hz frequency range. **Bottom:** 10 Hz only effects of spatial predictability (left), temporal predictability (center), and the interaction between these terms with gray shaded ranges indicating significance while controlling for a maximum false discovery rate (FDR) of 5%.  $S+/-$  refers to spatially unpredictable and predictable,  $T+/-$  to temporally unpredictable and predictable. Time axes indicate total trial time after the initial fixation cross with 0.4 seconds corresponding to the first entrainer.

centered around 5 Hz. This frequency was identified based on exploratory analysis and was also motivated by alternative models of sensory prediction (e.g., Arnal & Giraud, 2012; Giraud & Poeppel, 2012). Power and ITC at 5 Hz are plotted in Figures 3.10-3.11.

Both spatial and temporal predictability had a significant effect on 5 Hz power during the 200 ms blank period preceding the probe. Temporal predictability had a suppressive effect on 5 Hz

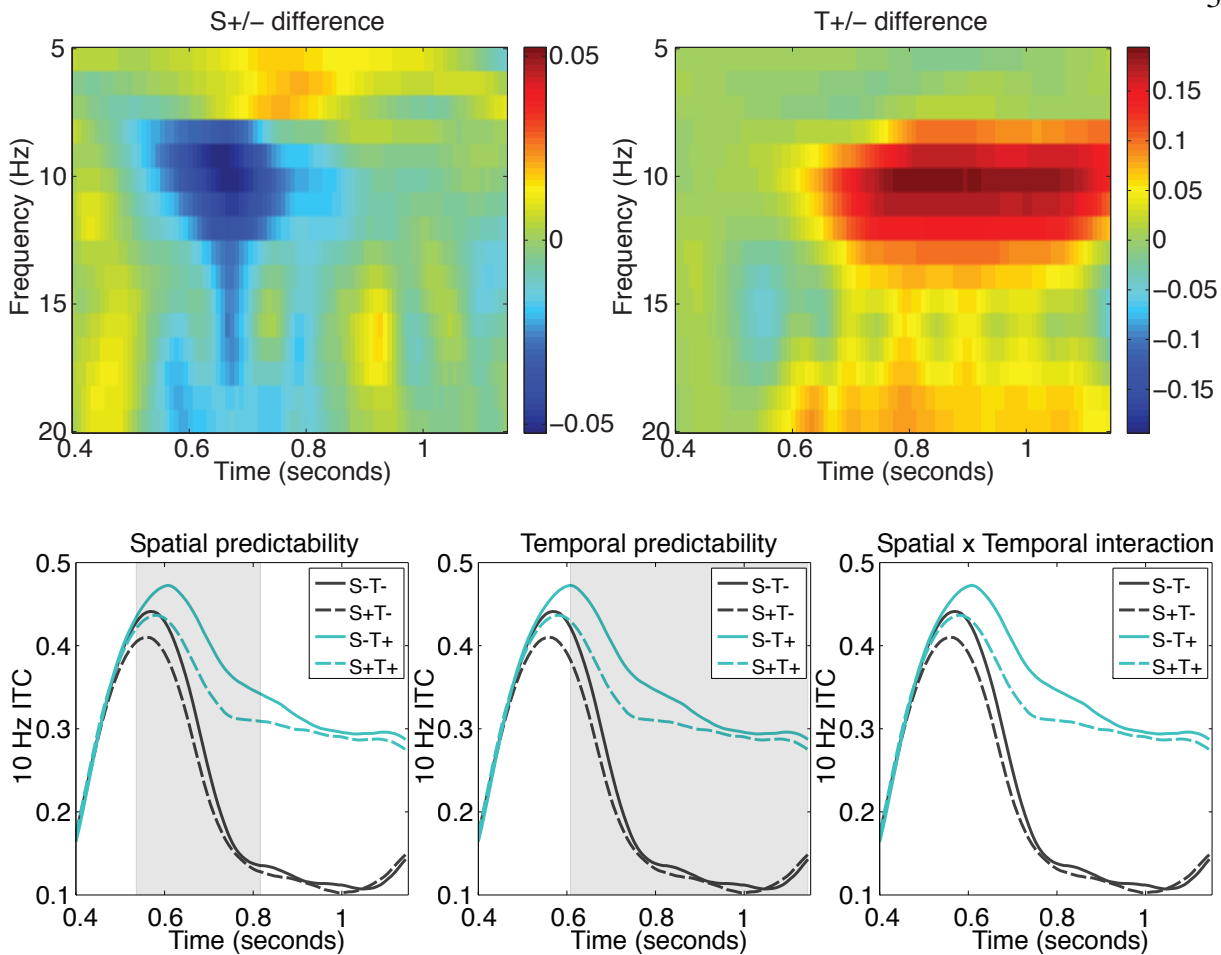


Figure 3.8: Effect of entrainer predictability on alpha phase coherence

Alpha-band inter-trial coherence (ITC) over the entraining sequence. Axes, legends, and shading for significant regions are the same as those described in Figure 3.7.

power, in contrast to the positive modulation found for 10 Hz power. This effect reversed following the presentation of the probe and persisted for over 300 ms. The interaction between spatial and temporal predictability failed to reach significance for 5 Hz power at any time points.

Temporal predictability also had a significant effect on 5 Hz ITC beginning during the 200 ms blank period preceding the probe and lasting nearly 300 ms after the presentation of the probe. Whereas 10 Hz ITC decreased during the blank period (yet remained significantly higher for temporally predictable stimuli), 5 Hz ITC increased, and continued to increase until approximately 100 ms after the onset of the probe. 5 Hz ITC was highest for the combined spatial and temporal

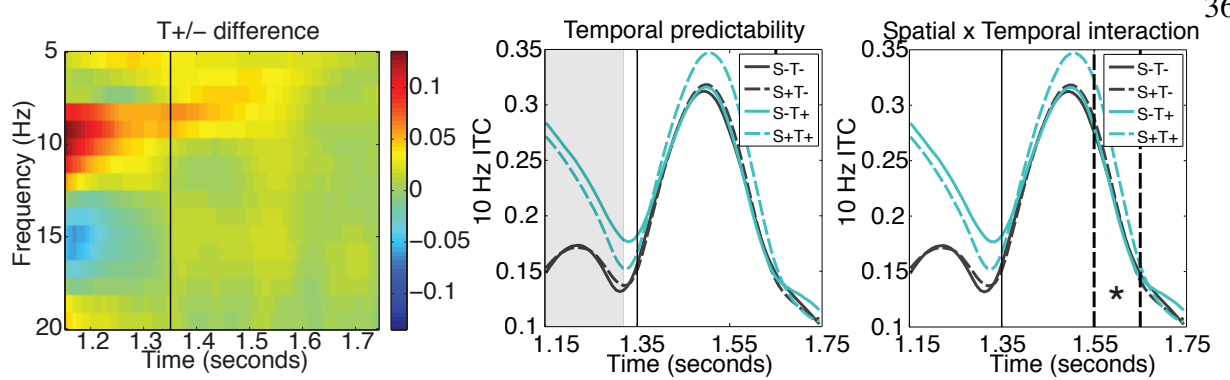


Figure 3.9: Alpha phase coherence before and after probe

Alpha-band inter-trial coherence (ITC) 200 ms preceding the probe and 400 ms following. Solid vertical line indicates probe onset. Asterisk indicates trending significance at the 5% level when averaging 10 Hz ITC within the window defined by the dotted lines. Time axes indicate total trial time after the initial fixation cross.

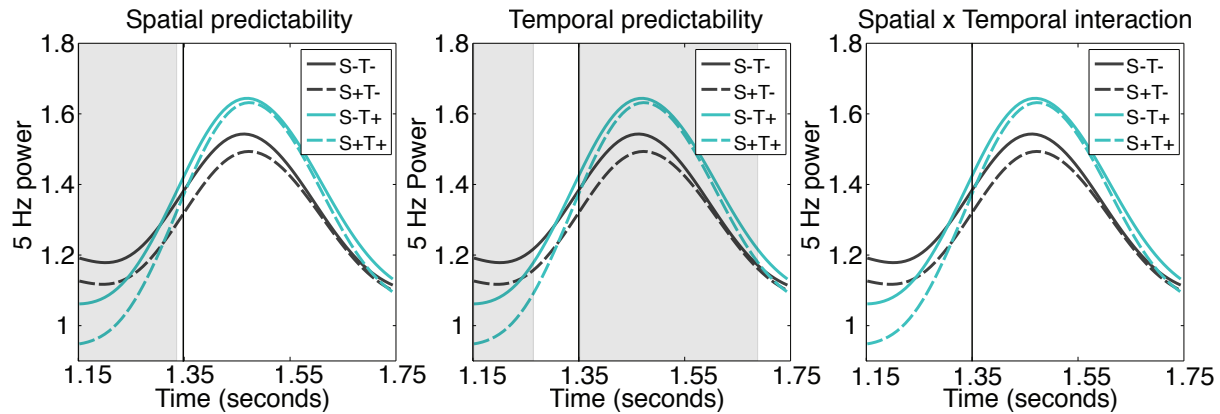


Figure 3.10: Delta-theta power before and after probe

Delta-theta power 200 ms preceding the probe and 400 ms following. Axes, legends, and shading for significant regions are the same as those described in Figure 3.9.

predictability condition (S+T+), indexed by a significant interaction beginning before the probe onset (-78 ms pre-stimulus) and persisting 154 ms after.

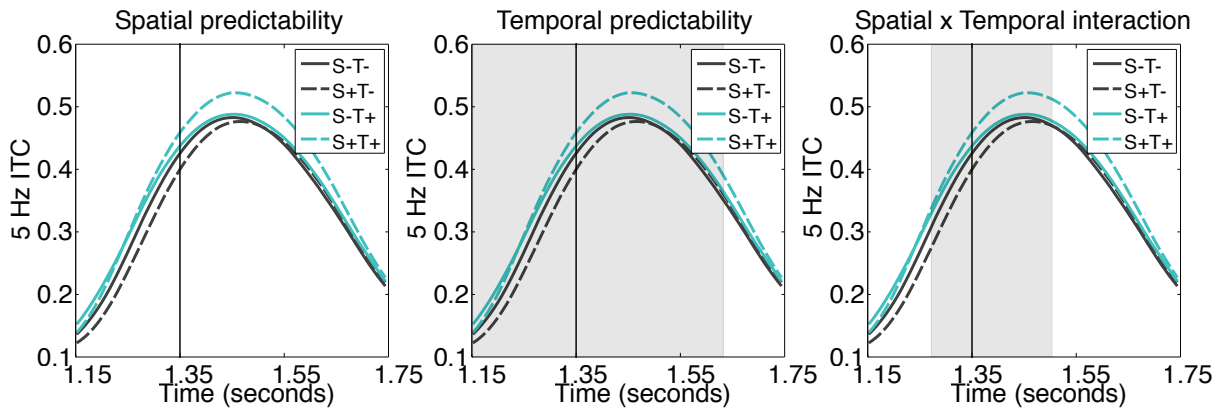


Figure 3.11: Delta-theta phase coherence before and after probe

Delta-theta inter-trial coherence (ITC) 200 ms preceding the probe and 400 ms following. Axes, legends, and shading for significant regions are the same as those described in Figure 3.9.

### 3.4 Discussion

#### 3.4.1 Summary of results

The work described in this chapter investigated how the brain integrates information from 100 ms samples and uses it to drive predictions about what will happen. The experimental paradigm used to address this question involved entraining alpha oscillatory activity to determine the effects of spatial and temporal predictability on a novel object recognition task. Behaviorally, there were robust effects of temporal predictability on raw accuracy and reaction times, as well as transformations to  $d'$ , a measure of sensitivity that takes into account response bias, and inverse efficiency, a measure that combines accuracy and reaction times (Townshend & Ashby, 2005). Accuracy was higher and response times were faster for a same-different judgement when entraining stimuli were presented in a temporally predictable manner. Spatial predictability was only significant for  $d'$  scores with higher sensitivity between “same” and “different” probes when entraining stimuli were presented in a predictable order, suggesting that raw accuracy might have been contaminated by response bias. Inverse efficiency, which can be thought of as the amount of energy consumed by the system to produce a behavioral outcome (Townshend & Ashby, 1983), was lower for tem-

porally predictable stimuli on average, but exhibited an increase for combined spatial and temporal predictability.

Event-related analysis of EEG data indicated that temporal predictability causes a strong periodicity (in this case, 10 Hz) phase aligned approximately to the onset of each temporally predictable entraining stimulus. This alignment approximately 180 degrees out of phase for temporally unpredictable stimuli and these differences in waveform alignment caused amplitude differences that preceded both entraining stimuli and the probe. The effects of spatial predictability generally manifested during the presentation of stimuli. There was an early divergence of probe-evoked activity caused by spatially predictable ordering of entrainers that over 100 ms through the P1 response with several transient effects after. There was evidence that spatial predictability was only effective when stimuli were also temporally predictable. This was evident for entrainers, and over right hemisphere channels during the probe. The effect failed to reach significance for left hemisphere channels and only trended toward significant levels when both hemispheres were considered jointly. It is likely that this is simply an issue of insufficient power, but other explanations such as hemispheric specialization (e.g., Dien09b) cannot be completely ruled out.

Both spatial and temporal predictability had effects on the power and phase coherence (indexed by inter-trial coherence, ITC) of neural oscillations. Spatially predictable entrainment caused a suppression of 10 Hz power with a lower degree of phase alignment than spatially random stimuli. Temporally predictable entrainment had the opposite effect, with increased 10 Hz power and phase alignment. Phase alignment due to temporal predictability remained elevated compared to temporally unpredictable stimuli during a 200 ms blank period between the entraining sequence and probe, indicating phase alignment could persist without exogenous entrainment. There was evidence of selective an enhancement in phase alignment for the combined spatial and temporal predictability case. As was the case in event-related analyses, this effect was significant in the right hemisphere, but not the left, and trended toward significance when both hemispheres were considered jointly. Power and phase coherence effects were also examined in the delta-theta bands (5 Hz) during the probe judgement. Results were similar to those found for 10 Hz, but more robust

with effects for both power and phase alignment.

### **3.4.2 Separate time courses for spatial and temporal prediction**

Spatial and temporal predictability were characterized by distinct and generally non-overlapping time courses. Temporal predictability manifested solely before (or at) the onset of each stimulus and appeared to be driven by an approximate antiphase relationship between temporally predictable and unpredictable stimuli. Spatial predictability generally manifested during the presentation of stimuli, although in the case of the probe, showed transient difference without stimulation. Predictability effects were similar for entraining stimuli and the probe except that the effect of spatial predictability persisted for over 100 ms through the P1 response with several more transient effects after. The similarity between entrainers and the probe suggests that the brain might treat the probe as a continuation of the entraining sequence and process it in the same manner.

From these results, we can conclude that temporal prediction is an anticipatory process, occurring during the absence of exogenous stimulation (in between entrainers or before the probe). The effect of temporal predictability extends 16 ms after the onset of each entrainer, but latencies for the first wave of responses in primary visual cortex (V1) are approximately 40-60 ms (NowakBullier97FoxeSimpson02) so there is no exogenous stimulation *per se* during the duration of the effect despite the stimulus being onscreen. Spatial prediction begins shortly before exogenous stimulation, but in the case of the probe, persists through the initial V1 responses. Spatial prediction, thus, might better be characterized as a post-stimulus process opposed to truly anticipatory process. The computation might involve a comparison between what is expected and what is actually coded by incoming spikes, consistent with the LeabraTI model (Chapter 2) as well as predictive coding models (e.g., RaoBallard99).

### **3.4.3 Oscillatory mechanisms of spatial and temporal prediction**

Spatial and temporal predictability had effects on both power and phase coherence of neural oscillations. In both cases, predictability took 2-3 entraining stimuli to establish, consistent

with previous investigations (MathewsonFabianiGrattonEtAl10; MathewsonPrudhommeFabiani-EtAl12). Spatial predictability was then characterized by a suppression of 10 Hz power and a phase angle variability causing a lower degree of alignment than spatially random stimuli. This effect is opposite than that of temporal predictability, which was characterized by increased 10 Hz power and phase angle alignment. Previous investigations have generally not simultaneously manipulated temporal rhythmicity and spatial coherence (although see Doherty et al., 2005) and thus, the relative suppression and decreased phase coherence during spatially predictable entrainment were unexpected results.

Successful oscillatory entrainment is thought to be a result of repeated phase resetting of endogenous oscillations causing phase to move into alignment with the frequency of exogenous stimulation (SchroederLakatosKajikawaEtAl08CalderoneLakatosButlerEtAlInPress). Oscillatory phase resetting has been shown to be caused by salient, unexpected events (FiebelkornFoxeButlerEtAl11; LandauFries12RomeiGrossThut12) and thus these unexpected results might be accounted for by considering successive views in terms of the amount of “surprise” (IttiBaldi09MeyerOlson11) they evoke. Subsequent views of the entraining sequence have significant feature overlap, characterized by the same populations of neurons spiking from one view to the next. Repeated spiking, especially as a function of expectation, has been shown to evoke rate suppression mechanisms (SummerfieldTritschuhMontiEtAl08). When entraining views are presented out of order, feature overlap is minimized and each view is “surprising”, causing an initial fast spiking burst response, which could lead to a higher degree of phase resetting.

The entrainment effects of spatial predictability were transient and dissipated before the end of the entraining sequence whereas the effects of temporal predictability persisted much longer. This might account for the null effects of spatial predictability on most behavioral measures. Temporal predictability effects persisted through the 200 ms blank period between the entraining sequence and probe and had robust effects on all behavioral measures. Thus, the present experiment could be modified to use a shorter entrainment sequence which would likely elicit successful spatial predictability for probe judgements.

The enhancement of 10 Hz phase angle alignment after the probe was presented did not reach significant levels assuming the FDR-corrected significance test at each time bin but did for 5 Hz phase alignment. Furthermore, temporal and spatial predictability main effects around the probe onset were more pronounced for 5 Hz oscillatory properties. One potential explanation for these effects is that reason for this is that the 200 ms blank period between the entraining sequence and the probe corresponded to two cycles at 10 Hz, but only one cycle at 5 Hz. Phase angles at 10 Hz exhibited significant dealignment over this period, and actually increased in alignment at 5 Hz. Thus, it is possible that this increase in phase alignment lead to a more pronounced selective enhancement for combined spatial predictability at 5 Hz, consisted with recent data (CravoRohenkohlWyartEtAl13). A more robust effect might be found for 10 Hz if the blank period between the entraining sequence and probe was only 100 ms in duration.

Another limitation of the present experimental paradigm is that it is unclear whether exogenous entrainment simply created new oscillations akin to steady state visually evoked potentials (SSVEP), or actually entrained existing endogenous oscillations. Thus, it might not be particularly surprising that temporally predictable stimuli caused increases in power and phase alignment. However, entrained alpha-band periodicity has been shown to correlate with individual resting alpha oscillation frequency (DeGraafGrossPatersonEtAl13) so it is likely that the paradigm recruited existing oscillations and caused them to align to the exogenous entrainment frequency. The fact that phase alignment continued through the 200 ms blank period without exogenous entrainment also supports this claim.

### **3.4.4 Prediction is not simply attentional orienting**

TODO after writing intro

### 3.4.5 Why does combined spatial and temporal predictability increase inverse efficiency?

#### References

- Armstrong-James, M., Fox, K., & Das-Gupta, A. (1992). Flow of excitation within rat barrel cortex on striking a single vibrissa. *Journal of Neurophysiology*, *68*(4), 1345–1358.
- Arnal, L. H., & Giraud, A.-L. (2012). Cortical oscillations and sensory predictions. *Trends in Cognitive Sciences*, *16*(7), 390–398.
- Balas, B. J., & Sinha, P. (2009). The role of sequence order in determining view canonicality for novel wire-frame objects. *Attention, Perception & Psychophysics*, *71*(4), 712–723.
- Benjamini, Y., & Yekutieli, D. (2001). The control of the false discovery rate in multiple testing under dependency. *The Annals of Statistics*, *29*(4), 1165–1188.
- Brainard, D. (1997). The Psychophysics Toolbox. *Spatial Vision*, *10*(4), 433–436.
- Buffalo, E. A., Fries, P., Landman, R., Buschman, T. J., & Desimone, R. (2011). Laminar differences in gamma and alpha coherence in the ventral stream. *Proceedings of the National Academy of Sciences of the United States of America*, *108*(27), 11262–11267.
- Bulthoff, H. H., & Edelman, S. (1992). Psychophysical support for a two-dimensional view interpolation theory of object recognition. *Proceedings of the National Academy of Sciences of the United States of America*, *89*(1), 60–64.
- Busch, N. A., Dubois, J., & VanRullen, R. (2009). The phase of ongoing EEG oscillations predicts visual perception. *The Journal of Neuroscience*, *29*(24), 7869–7876.
- Buxhoeveden, D. P., & Casanova, M. F. (2002). The minicolumn hypothesis in neuroscience. *Brain*, *125*(Pt 5), 935–951.
- Connors, B. W., Gutnick, M. J., & Prince, D. A. (1982). Electrophysiological properties of neocortical neurons in vitro. *Journal of Neurophysiology*, *48*(6), 1302–1320.
- Cousineau, D. (2005). Confidence intervals in within-subject designs: A simpler solution to Loftus and Massons method. *Tutorials in Quantitative Methods for Psychology*, *1*(1), 42–45.
- Delorme, A., & Makeig, S. (2004). EEGLAB: An open source toolbox for analysis of single-trial EEG dynamics including independent component analysis. *Journal of Neuroscience Methods*, *134*(1), 9–21.
- Doherty, J. R., Rao, A., Mesulam, M. M., & Nobre, A. C. (2005). Synergistic effect of combined temporal and spatial expectations on visual attention. *The Journal of Neuroscience*, *25*(36), 8259–8266.
- Douglas, R. J., & Martin, K. A. C. (2004). Neuronal circuits of the neocortex. *Annual Review of Neuroscience*, *27*, 419–451.
- Edelman, S., & Bulthoff, H. H. (1992). Orientation dependence in the recognition of familiar and novel views of three-dimensional objects. *Vision Research*, *32*(12), 2385–2400.
- Elman, J. L. (1990). Finding structure in time. *Cognitive Science*, *14*(2), 179–211.

- Fahrenfort, J. J., Scholte, H. S., & Lamme, V. A. F. (2007). Masking disrupts reentrant processing in human visual cortex. *Journal of Cognitive Neuroscience*, *19*(9), 1488–1497.
- Felleman, D. J., & Van Essen, D. C. (1991). Distributed hierarchical processing in the primate cerebral cortex. *Cerebral Cortex*, *1*(1), 1–47.
- Foldiak, P. (1991). Learning invariance from transformation sequences. *Neural Computation*, *3*(2), 194–200.
- Franceschetti, S., Guatteo, E., Panzica, F., Sancini, G., Wanke, E., & Avanzini, G. (1995). Ionic mechanisms underlying burst firing in pyramidal neurons: Intracellular study in rat sensorimotor cortex. *Brain Research*, *696*(1–2), 127–139.
- Giraud, A.-L., & Poeppel, D. (2012). Cortical oscillations and speech processing: Emerging computational principles and operations. *Nature Neuroscience*, *15*(4), 511–517.
- Hirsch, J. A., & Martinez, L. M. (2006). Laminar processing in the visual cortical column. *Current Opinion in Neurobiology*, *16*(4), 377–384.
- Horton, J. C., & Adams, D. L. (2005). The cortical column: A structure without a function. *Philosophical Transactions of the Royal Society B*, *360*(1456), 837–862.
- Hubel, D. H., & Wiesel, T. N. (1977). Ferrier lecture. Functional architecture of macaque monkey visual cortex. *Proceedings of the Royal Society B*, *198*(1130), 1–59.
- Hughes, S. W., Lorincz, M., Cope, D. W., Blethyn, K. L., Kekesi, K. A., Parri, H. R., Juhasz, G., & Crunelli, V. (2004). Synchronized oscillations at alpha and theta frequencies in the lateral geniculate nucleus. *Neuron*, *42*(2), 253–268.
- Jones, E. G. (2000). Microcolumns in the cerebral cortex. *Proceedings of the National Academy of Sciences of the United States of America*, *97*(10), 5019–5021.
- Lachaux, J. P., Rodriguez, E., Martinerie, J., & Varela, F. J. (1999). Measuring phase synchrony in brain signals. *Human Brain Mapping*, *8*(4), 194–208.
- Lakatos, P., Karmos, G., Mehta, A. D., Ulbert, I., & Schroeder, C. E. (2008). Entrainment of neuronal oscillations as a mechanism of attentional selection. *Science*, *320*(5872), 110–113.
- Logothetis, N., Pauls, J., Bulthoff, H., & Poggio, T. (1994). View-dependent object recognition by monkeys. *Current Biology*, *4*(5), 401–414.
- Logothetis, N. K., Pauls, J., & Poggio, T. (1995). Shape representation in the inferior temporal cortex of monkeys. *Current Biology*, *5*(5), 552–563.
- Lopes da Silva, F. (1991). Neural mechanisms underlying brain waves: from neural membranes to networks. *Electroencephalography and Clinical Neurophysiology*, *79*(2), 81–93.
- Lorincz, M. L., Crunelli, V., & Hughes, S. W. (2008). Cellular dynamics of cholinergically induced alpha (8-13 hz) rhythms in sensory thalamic nuclei in vitro. *The Journal of Neuroscience*, *28*(3), 660–671.
- Lorincz, M. L., Kekesi, K. A., Juhasz, G., Crunelli, V., & Hughes, S. W. (2009). Temporal framing of thalamic relay-mode firing by phasic inhibition during the alpha rhythm. *Neuron*, *63*(5), 683–696.

- Luczak, A., Bartho, P., & Harris, K. D. (2013). Gating of sensory input by spontaneous cortical activity. *The Journal of Neuroscience*, *33*(4), 1684–1695.
- Lumer, E., Edelman, G., & Tononi, G. (1997). Neural dynamics in a model of the thalamocortical system. I. Layers, loops and the emergence of fast synchronous rhythms. *Cerebral Cortex*, *7*(3), 207–227.
- Masquelier, T., & Thorpe, S. J. (2007). Unsupervised learning of visual features through spike timing dependent plasticity. *PLoS Computational Biology*, *3*(2), 247–257.
- Mathewson, K. E., Lleras, A., Beck, D. M., Fabiani, M., Ro, T., & Gratton, G. (2011). Pulsed out of awareness: EEG alpha oscillations represent a pulsed-inhibition of ongoing cortical processing. *Frontiers in Psychology*, *2*.
- Mountcastle, V. B. (1997). The columnar organization of the neocortex. *Brain*, *120*(Pt 4), 701–722.
- Mutch, J., & Lowe, D. (2008). Object class recognition and localization using sparse features with limited receptive fields. *International Journal of Computer Vision*, *80*(1), 45–57.
- Oostenveld, R., Fries, P., Maris, E., & Schoffelen, J.-M. (2011). FieldTrip: Open source software for advanced analysis of MEG, EEG, and invasive electrophysiological data. *Computational Intelligence and Neuroscience*, *2011*.
- O'Reilly, R. C., & Munakata, Y. (2000). *Computational Explorations in Cognitive Neuroscience: Understanding the Mind by Simulating the Brain*. Cambridge, MA: The MIT Press.
- O'Reilly, R. C., Munakata, Y., Frank, M. J., Hazy, T. E., & Contributors (2012). *Computational Cognitive Neuroscience*. Wiki Book, 1st Edition, URL: <http://ccnbook.colorado.edu>.
- Pelli, D. (1997). The VideoToolbox software for visual psychophysics: Transforming numbers into movies. *Spatial Vision*, *10*(4), 437–442.
- Perrin, F., Pernier, J., Bertrand, O., & Echallier, J. F. (1989). Spherical splines for scalp potential and current density mapping. *Electroencephalography and Clinical Neurophysiology*, *72*(2), 184–187.
- Rockland, K. S., & Pandya, D. N. (1979). Laminar origins and terminations of cortical connections of the occipital lobe in the rhesus monkey. *Brain Research*, *179*(1), 3–20.
- Rohenkohl, G., & Nobre, A. C. (2011). Alpha oscillations related to anticipatory attention follow temporal expectations. *The Journal of Neuroscience*, *31*(40), 14076–14084.
- Schroeder, C. E., & Lakatos, P. (2009). Low-frequency neuronal oscillations as instruments of sensory selection. *Trends in Neurosciences*, *32*(1), 9–18.
- Serre, T., Oliva, A., & Poggio, T. (2007). A feedforward architecture accounts for rapid categorization. *Proceedings of the National Academy of Sciences of the United States of America*, *104*(15), 6424–6429.
- Servan-Schreiber, D., Cleeremans, A., & McClelland, J. L. (1991). Graded state machines: The representation of temporal contingencies in simple recurrent networks. *Machine Learning*, *7*(2–3), 161–193.

- Silva, L. R., Amitai, Y., & Connors, B. W. (1991). Intrinsic oscillations of neocortex generated by layer 5 pyramidal neurons. *Science*, *251*(4992), 432–435.
- Sinha, P., & Poggio, T. (1996). Role of learning in three-dimensional form perception. *Nature*, *384*(6608), 460–463.
- Spaak, E., Bonnefond, M., Maier, A., Leopold, D. A., & Jensen, O. (2012). Layer-specific entrainment of gamma-band neural activity by the alpha rhythm in monkey visual cortex. *Current Biology*, *22*(24), 2313–2318.
- Stefanics, G., Hangya, B., Herndi, I., Winkler, I., Lakatos, P., & Ulbert, I. (2010). Phase entrainment of human delta oscillations can mediate the effects of expectation on reaction speed. *The Journal of Neuroscience*, *30*(41), 13578–13585.
- Thomson, A. M. (2010). Neocortical layer 6, a review. *Frontiers in Neuroanatomy*, *4*.
- Thomson, A. M., & Lamy, C. (2007). Functional maps of neocortical local circuitry. *Frontiers in Neuroscience*, *1*(1), 19–42.
- Townshend, J. T., & Ashby, F. G. (1983). *Stochastic Modeling of Elementary Psychological Processes*. Cambridge: Cambridge University Press.
- Townshend, J. T., & Ashby, F. G. (2005). Methods of modeling capacity in simple processing systems. In J. N. Castellan Jr., & F. Restle (Eds.), *Cognitive Theory: Volume 3* (pp. 200–239). Hillsdale, NJ: Lawrence Erlbaum Associates.
- VanRullen, R., Busch, N. A., Drewes, J., & Dubois, J. (2011). Ongoing EEG phase as a trial-by-trial predictor of perceptual and attentional variability. *Frontiers in Psychology*, *2*.
- Will, U., & Berg, E. (2007). Brain wave synchronization and entrainment to periodic acoustic stimuli. *Neuroscience letters*, *424*(1), 55–60.

## **Chapter 4**

### **Effects of spatial and temporal prediction during novel object learning**

#### **4.1 Introduction**

TODO

#### **4.2 Methods**

##### **4.2.1 Participants**

A total of 62 students from the University of Colorado Boulder participated in the experiment (ages 18-22, mean=19.11 years; 30 male, 32 female). All participants reported normal or corrected-to-normal vision and received course credit as compensation for their participation. Informed consent was obtained from each participant prior to the experiment in accordance with Institutional Review Board policy at the University of Colorado.

##### **4.2.2 Stimuli**

Novel “paper clip” objects were used as stimuli (see Chapter 3 Methods). A total of eight objects were used – four as targets and four as distractors. The four target objects were also used in the experiment described in Chapter 3. Target and distractor objects were paired together for the purposes of the experiment. All objects are shown in Figure 4.1.

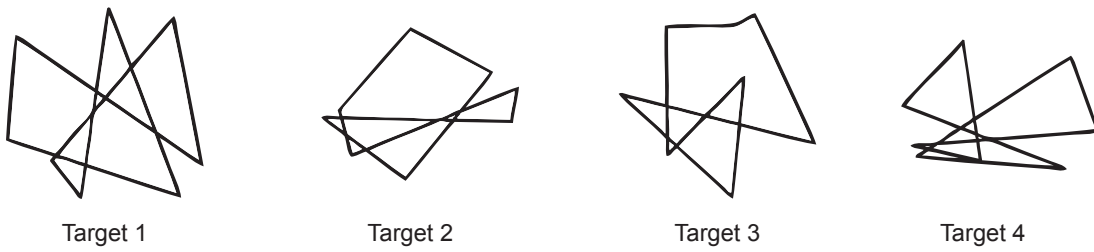
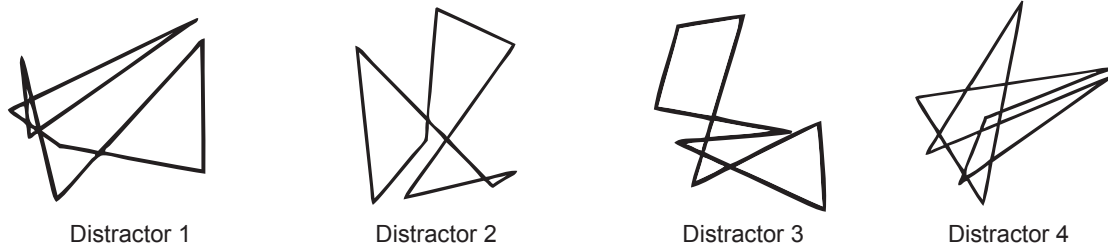
**A****B**

Figure 4.1: Novel “paper clip” objects

Four target (**A**) and four distractor object pairs (**B**) used in the experiment. See Chapter 3 Methods for additional information.

#### 4.2.3 Procedure

The experiment was divided into 16 blocks, each containing a training period followed by a series of test trials (Figure 4.2). During the training period of a given block, participants observed one of the target objects rotate about its y-axis. The object either rotated coherently (i.e., spatially predictable, S+ conditions) or in a random manner (S- conditions). Coherent rotation was composed of adjacent views spaced 12 degrees apart. The object made four complete rotations during the study period. All views of the object were still presented four times each in the random case. The presentation rate during the study period was either 10 Hz with a 50 ms on time and 50 ms off time (i.e., temporally predictable, T+ conditions) or variable with a 50 ms on time and off times ranging from 16.67-400 ms (T- conditions).

The S+/- and T+/- conditions were crossed and each of the target-distractor object pairs was assigned to one of the four conditions. These assignments were approximately counterbalanced across participants (Assignment 1:  $N=15$ ; Assignment 2:  $N=17$ ; Assignment 3:  $N=15$ ; Assignment

4:  $N=15$ ). Each block condition with its target-distractor pairing was repeated for four blocks during the experiment. Block order randomized was randomized for each participant.

During each block, participants were instructed to study the target object during the training period and then complete a series of 30 test trials. On each test trial, either the target object or its paired distractor was presented. Participants were instructed to respond “same” if they believed the object depicted the trained target object or “different” if they believed it depicted the distractor object. Half of the test trials contained 15 views of the target object spaced 24 degrees apart, and the other half contained 15 views of the distractor, also spaced 24 degrees apart. Test trials were shown in a random order and feedback was withheld to prevent participants from changing their response criteria over the course of a block.

The experiment was displayed on an LCD monitor at native resolution operating at 60 Hz using the Psychophysics Toolbox Version 3 (Brainard, 1997; Pelli, 1997). All stimuli were presented on an isoluminant 50% gray background and subtended approximately 5 degrees of visual angle. Test trials began with a fixation cross (200 ms) followed by a blank (400 ms) followed by the probe stimulus (100 ms). Participants were required to respond within 2000 ms. Subsequent test trials were separated by a variable intertrial interval of 1000-1400 ms.

The experiment began with a practice block to ensure that participants understood the task. The training period during the practice block was always spatially and temporally predictable and used a reserved target object and distractor that were not further used in any of the experimental blocks. During the practice test trials, participants received feedback after responding according to whether they were correct or incorrect. After completing the practice block, participants were informed that future training periods could be presented in spatially and/or temporally unpredictable manners.

### 4.3 Results

Three subjects were excluded from behavioral analysis for accuracy  $2.7\sigma$  (or further) below mean accuracy across subjects. All three excluded subjects were assigned condition-object 3 re-

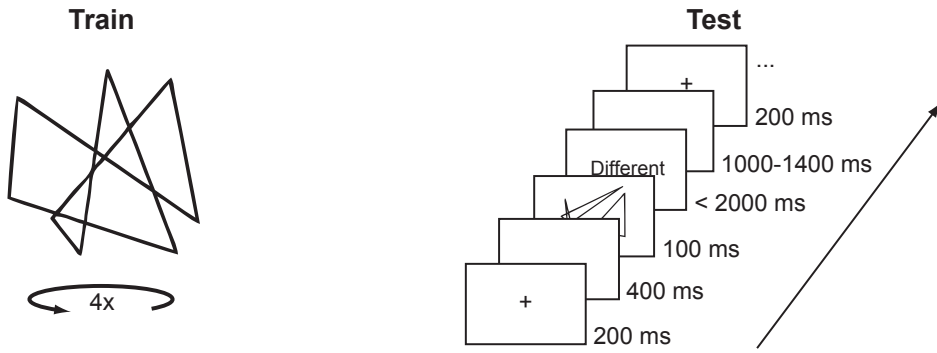


Figure 4.2: Experimental procedure

Experimental trials were composed of a training period followed by a testing period. The training period depicted a target object rotating a total of four times around its vertical axis. Rotation was either spatially and temporally predictable, spatially predictable or temporally predictable only, or completely unpredictable. The test period contained 30 trials that depicted either the training object or its paired distractor at 15 viewing angles each.

sulting in the final counterbalancing – Assignment 1:  $N=15$ ; Assignment 2:  $N=14$ ; Assignment 3:  $N=15$ ; Assignment 4:  $N=15$ . The remaining 59 subjects were submitted to a  $2 \times 2$  ANOVA with spatial and temporal predictability as within-subjects factors and counterbalancing assignment as a between-subjects factor. Accuracy and reaction times are plotted in Figure 4.3. Transformed behavioral measures (e.g.,  $d'$ , inverse efficiency; see Chapter 3 Results) showed similar patterns to the raw measures and are thus omitted from analysis.

Overall, subjects were less accurate when the training period was spatially predictable ( $F(1, 57) = 4.50, p = 0.038$ ) or temporally predictable ( $F(1, 57) = 4.20, p = 0.046$ ). The interaction between spatial and temporal predictability failed to reach significance ( $F(1, 57) = 0.20, p = 0.659$ ). Subjects were least accurate for the combined spatial and temporal predictability condition (denoted S+T+ in Figure 4.3). This condition significantly differed from the completely unpredictable condition (S-T-) ( $t(58) = -2.8587, p = 0.001$ ), and trended toward significance for conditions with only spatial or only temporal predictability (S+T+ versus S+T-,  $t(58) = -1.60, p = 0.116$ ; S-T- versus S+T+ versus S-T+,  $t(58) = -1.77, p = 0.082$ ).

Subjects were also slower to respond when the training period was spatially predictable ( $F(1,$

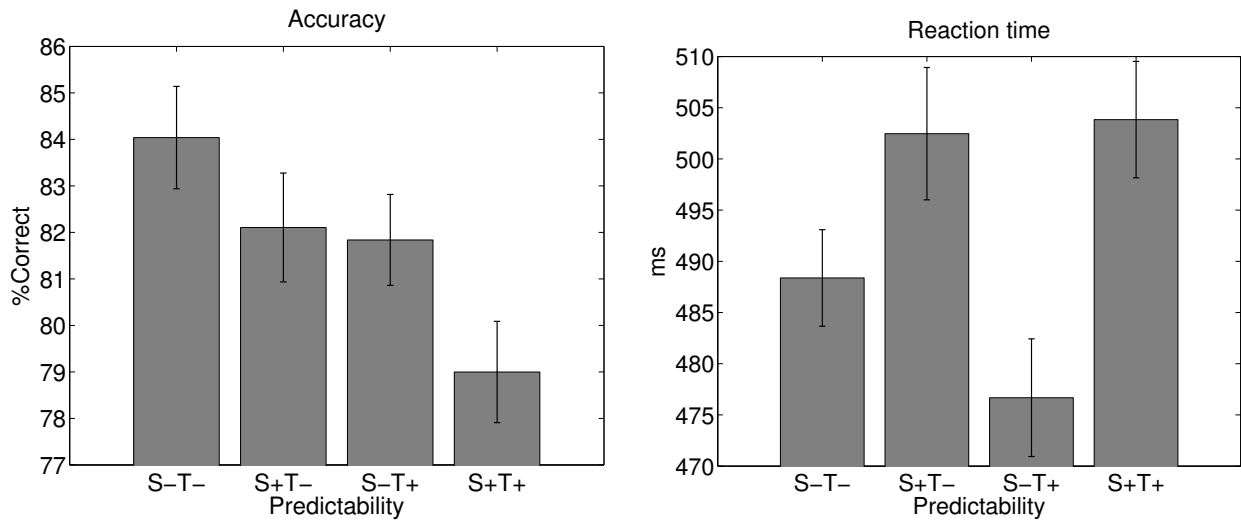


Figure 4.3: Behavioral measures of spatial and temporal predictability

Accuracy and reaction time as a function of predictability during the training period. S-/+ refers to spatially unpredictable and predictable, T-/+ to temporally unpredictable and predictable. Error bars depict within-subjects error using the method described in Cousineau (2005) adapted for standard error.

$F(1, 57) = 10.99, p = 0.002$ ). A similar effect for temporal predictability failed to reach significance ( $F(1, 57) = 0.53, p = 0.471$ ), nor did the interaction between spatial and temporal predictability ( $F(1, 57) = 1.21, p = 0.276$ ).

Effects were highly variable across target objects (Figure 4.4). Target-condition assignment did not significantly affect accuracy or reaction times (both  $p$ 's  $> 0.05$ ), but often interacted with predictability effects and their interactions. One reason for this variability regards the orthographic projection used to render the objects. Previous research has indicated that recognition accuracy fluctuates as a function of how well the two-dimensional projection of an object captures its full three-dimensional structure (Balas & Sinha, 2009). For example, when there is a large amount of foreshortening in the projection, it could be difficult to infer the length of line segments that compose the object, impairing recognition. These degenerate projections are generally diametrically opposed on the object.

Accuracy was computed as a function of viewing angle for each target object to investigate

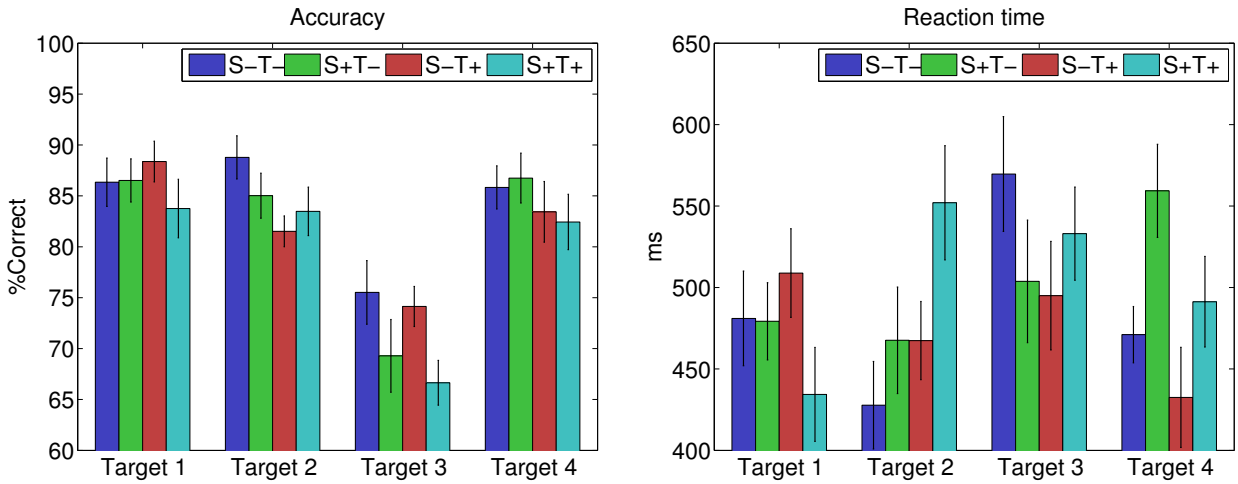


Figure 4.4: Behavioral measures for each target object

Accuracy and reaction times for each target object. Horizontal axes denote target and colors predictability during the training period. Error bars depict between-subjects standard error.

whether it interacted with predictability during the training period (Figure 4.5). Test trials during which distractor objects were presented were excluded from this analysis since there is no consistent relationship between the targets and distractors across viewing angles and thus they would only contribute noise. With the exception of target object 1, all objects indicated fluctuations in accuracy as a function of viewing angle with two diametrically opposed degenerate views. The most consistent differences in accuracy between training conditions appeared to be localized to the troughs of the accuracy function, corresponding to these degenerate views.

Standard statistical tests did not have enough power to detect differences between conditions for degenerate views because each data point corresponded to only four trials per subject. To address this design limitation, a bootstrapping method was used to resample the available data in these cases. The accuracy function over viewing angles was collapsed across conditions and the two minima associated with degenerate views were identified for each object. For target object 1, this corresponded to angles  $\theta = \{24^\circ, 312^\circ\}$ , object 2:  $\theta = \{48^\circ, 240^\circ\}$  object 3:  $\theta = \{144^\circ, 312^\circ\}$ , and object 4  $\theta = \{24^\circ, 192^\circ\}$ . Accuracy for the completely unpredictable (S-T-) and combined spatial and temporal predictability (S+T+) conditions during training was averaged at these viewing

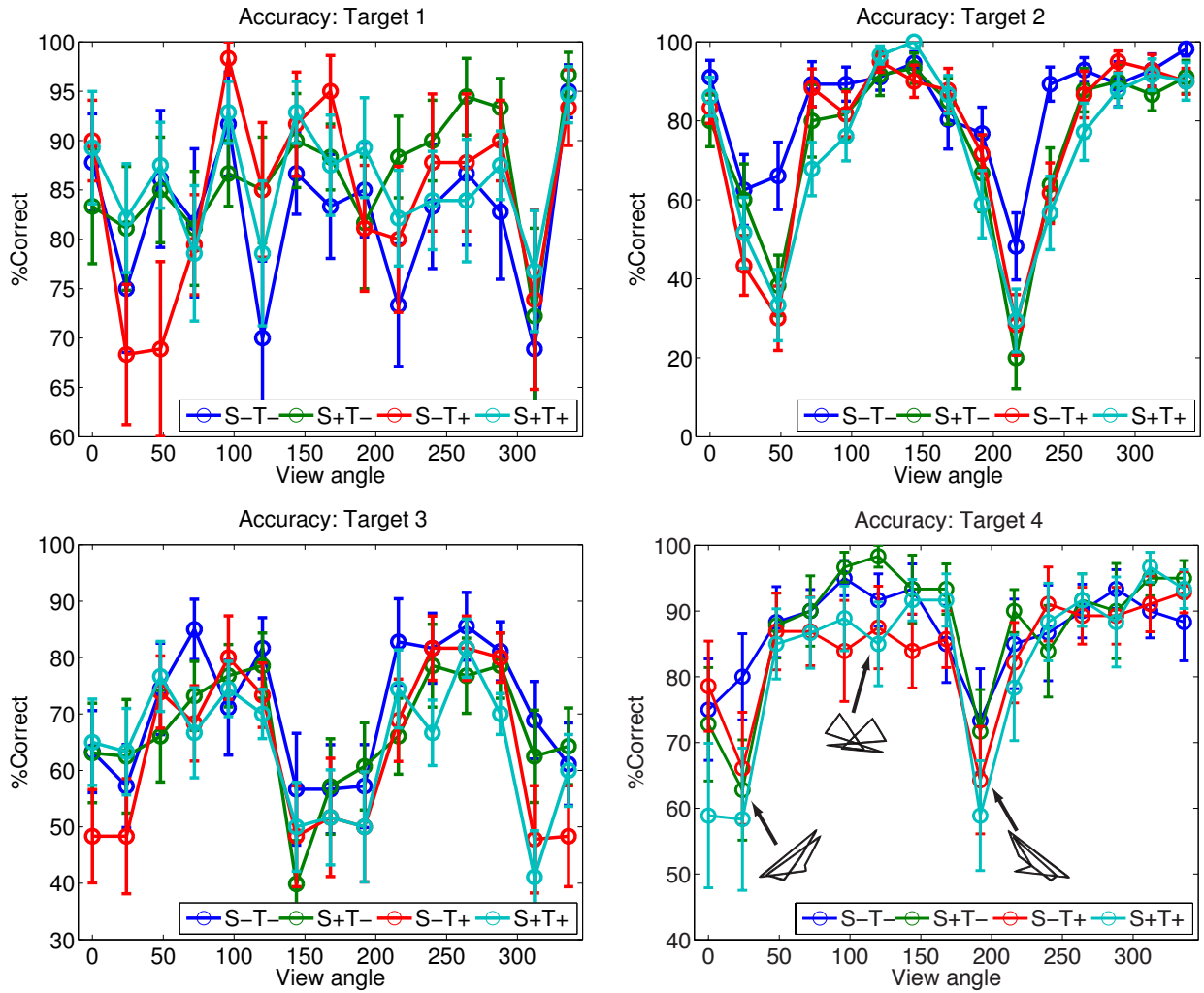


Figure 4.5: Accuracy as a function of viewing angle for each target object

Target accuracy at each viewing angle presented during the test periods. Horizontal axes denote viewing angle and colors predictability during the training period. Error bars depict between-subjects standard error. Diametrically opposed foreshortened views and one canonical view are shown for target object 4.

angles and resampled with replacement from the 59 subjects for 10000 iterations. This produced distributions for degenerate view accuracy for each object (Figure 4.6). Accuracy for was lower for degenerate views for the combined spatial and temporal predictability condition for all target objects except target 1, which didn't exhibit the patterned accuracy function that other targets did. The S+T+/S-T- difference in accuracy for degenerate views was significant at the 90% alpha level

(i.e., the confidence interval of the difference between means did not include zero) for all target objects except target 1.

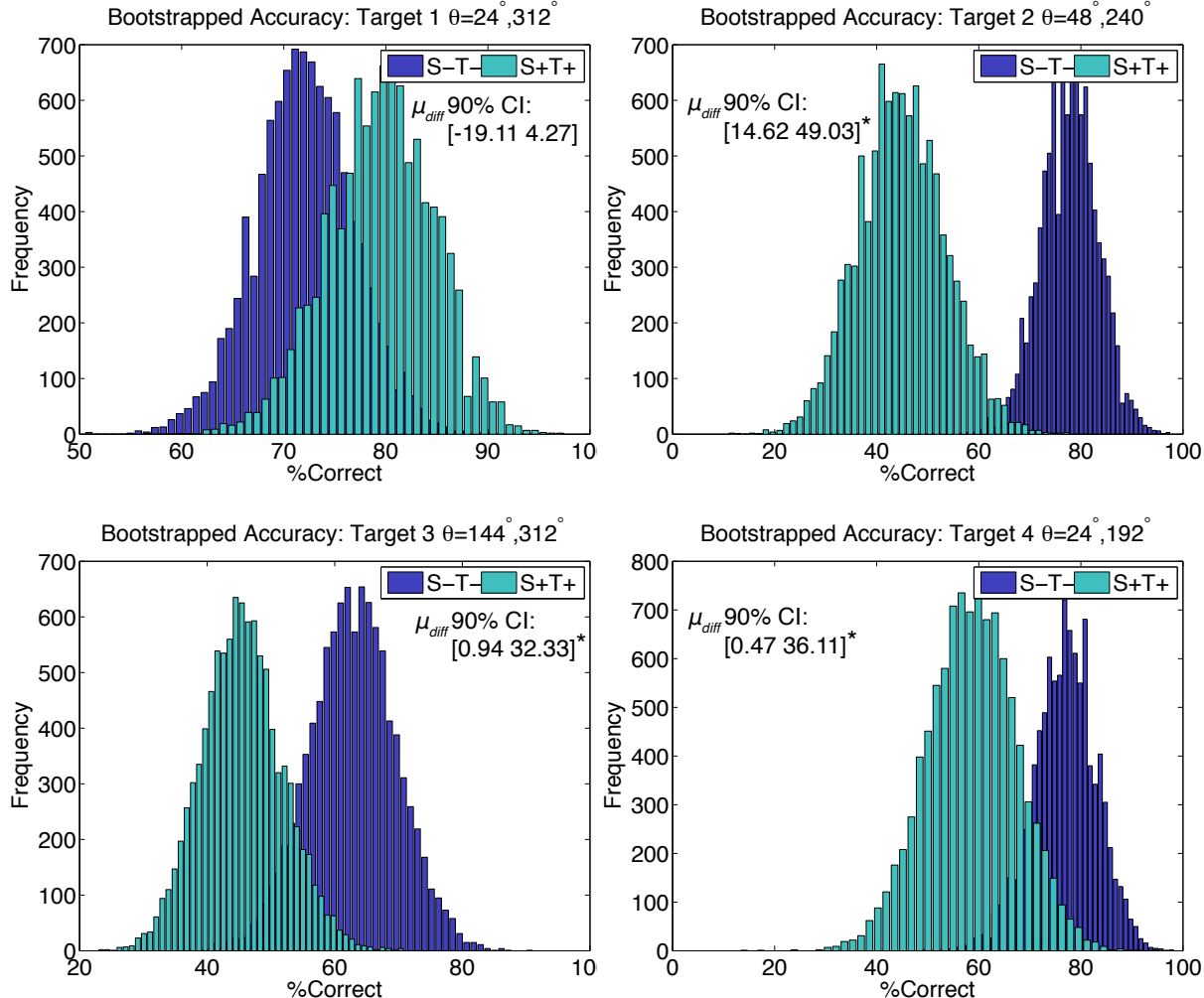


Figure 4.6: Bootstrapped accuracy for degenerate views

Average target accuracy for degenerate views resampled with replacement from the 59 subjects for 10000 iterations. Viewing angle for averaging is noted for each target object. Asterisks denote significant differences based on 90% confidence intervals.

## 4.4 Discussion

### 4.4.1 Summary of results

The work described in this chapter investigated how predictability biased learned representations of novel objects. The experimental paradigm used to address this question involved training participants to recognize novel objects while manipulating their spatial and temporal predictability. Somewhat surprisingly, accuracy was lowest when stimuli were learned in a combined spatially and temporally predictable context and highest when learned in a completely unpredictable context. Reaction times were also slower when objects were learned with spatial predictability.

Behavioral measures were highly variable across objects. There was some indication that differences between predictability conditions during training were driven primarily by degenerate viewing angles caused by three-dimensional foreshortening in the objects used. A foreshortening model has previously accounted for the principal component of variability in recognition accuracy for the same “paper clip” objects used here (Balas & Sinha, 2009), but only in a combined spatial and temporal predictability learning context.

### 4.4.2 A behavioral disadvantage for spatial prediction during object learning

Based on previous research, it is unclear whether spatial predictability is used by the brain during object learning and whether it is actually advantageous. Initial investigations described in LawsonHumphreysWatson94) identified the expected increase in recognition accuracy for spatially predictable sequences. The foreshortening model advanced in (Balas & Sinha, 2009) was also improved by incorporating spatial information (e.g., the first- and second-order derivatives of the foreshortening function over object views). Furthermore, a number of computational models, including LeabraTI (Chapter 2), use learning rules that incorporate associations between subsequent inputs to learn object representations (Foldiak, 1991StringerPerryRollsEtAl06WallisBaddeley97IsikLeiboPoggio12).

Experiments described in HarmanHumphrey99) failed to find any positive or negative effects of spatial predictability on accuracy. They did, however, increase in reaction time for objects

learned in a spatially predictable context, similar to the one reported here. One possible reason for the slowing of reaction times for objects learned with spatial predictability is that less attention is necessary in these conditions. A constantly changing sequence of views might require more attentive processing to encode whereas the relatively low amount of change between views in spatially predictable sequences is less “surprising” and some views might be overlooked during encoding. However, there was some indication that the adverse effect of spatial predictability was driven primarily by the degenerate views of the stimuli used in the present work. A more focused experiment would be necessary to explicitly test the hypothesis impaired for degenerate views learned in a spatially predictable context and relatively intact for canonical views, but the interpretation of this hypothesis if confirmed is still discussed here.

#### **4.4.3 Spatiotemporal prediction biases development of invariance**

The theory advanced here is that spatially predictable sequences promote learning of view-invariant object representations, whereas spatially unpredictable sequences promote learning view-dependent representations.

### **References**

- Armstrong-James, M., Fox, K., & Das-Gupta, A. (1992). Flow of excitation within rat barrel cortex on striking a single vibrissa. *Journal of Neurophysiology*, 68(4), 1345–1358.
- Arnal, L. H., & Giraud, A.-L. (2012). Cortical oscillations and sensory predictions. *Trends in Cognitive Sciences*, 16(7), 390–398.
- Balas, B. J., & Sinha, P. (2009). The role of sequence order in determining view canonicality for novel wire-frame objects. *Attention, Perception & Psychophysics*, 71(4), 712–723.
- Benjamini, Y., & Yekutieli, D. (2001). The control of the false discovery rate in multiple testing under dependency. *The Annals of Statistics*, 29(4), 1165–1188.
- Brainard, D. (1997). The Psychophysics Toolbox. *Spatial Vision*, 10(4), 433–436.
- Buffalo, E. A., Fries, P., Landman, R., Buschman, T. J., & Desimone, R. (2011). Laminar differences in gamma and alpha coherence in the ventral stream. *Proceedings of the National Academy of Sciences of the United States of America*, 108(27), 11262–11267.

- Bulthoff, H. H., & Edelman, S. (1992). Psychophysical support for a two-dimensional view interpolation theory of object recognition. *Proceedings of the National Academy of Sciences of the United States of America*, *89*(1), 60–64.
- Busch, N. A., Dubois, J., & VanRullen, R. (2009). The phase of ongoing EEG oscillations predicts visual perception. *The Journal of Neuroscience*, *29*(24), 7869–7876.
- Buxhoeveden, D. P., & Casanova, M. F. (2002). The minicolumn hypothesis in neuroscience. *Brain*, *125*(Pt 5), 935–951.
- Connors, B. W., Gutnick, M. J., & Prince, D. A. (1982). Electrophysiological properties of neocortical neurons in vitro. *Journal of Neurophysiology*, *48*(6), 1302–1320.
- Cousineau, D. (2005). Confidence intervals in within-subject designs: A simpler solution to Loftus and Massons method. *Tutorials in Quantitative Methods for Psychology*, *1*(1), 42–45.
- Delorme, A., & Makeig, S. (2004). EEGLAB: An open source toolbox for analysis of single-trial EEG dynamics including independent component analysis. *Journal of Neuroscience Methods*, *134*(1), 9–21.
- Doherty, J. R., Rao, A., Mesulam, M. M., & Nobre, A. C. (2005). Synergistic effect of combined temporal and spatial expectations on visual attention. *The Journal of Neuroscience*, *25*(36), 8259–8266.
- Douglas, R. J., & Martin, K. A. C. (2004). Neuronal circuits of the neocortex. *Annual Review of Neuroscience*, *27*, 419–451.
- Edelman, S., & Bulthoff, H. H. (1992). Orientation dependence in the recognition of familiar and novel views of three-dimensional objects. *Vision Research*, *32*(12), 2385–2400.
- Elman, J. L. (1990). Finding structure in time. *Cognitive Science*, *14*(2), 179–211.
- Fahrenfort, J. J., Scholte, H. S., & Lamme, V. A. F. (2007). Masking disrupts reentrant processing in human visual cortex. *Journal of Cognitive Neuroscience*, *19*(9), 1488–1497.
- Felleman, D. J., & Van Essen, D. C. (1991). Distributed hierarchical processing in the primate cerebral cortex. *Cerebral Cortex*, *1*(1), 1–47.
- Foldiak, P. (1991). Learning invariance from transformation sequences. *Neural Computation*, *3*(2), 194–200.
- Franceschetti, S., Guatteo, E., Panzica, F., Sancini, G., Wanke, E., & Avanzini, G. (1995). Ionic mechanisms underlying burst firing in pyramidal neurons: Intracellular study in rat sensorimotor cortex. *Brain Research*, *696*(1–2), 127–139.
- Giraud, A.-L., & Poeppel, D. (2012). Cortical oscillations and speech processing: Emerging computational principles and operations. *Nature Neuroscience*, *15*(4), 511–517.
- Hirsch, J. A., & Martinez, L. M. (2006). Laminar processing in the visual cortical column. *Current Opinion in Neurobiology*, *16*(4), 377–384.
- Horton, J. C., & Adams, D. L. (2005). The cortical column: A structure without a function. *Philosophical Transactions of the Royal Society B*, *360*(1456), 837–862.
- Hubel, D. H., & Wiesel, T. N. (1977). Ferrier lecture. Functional architecture of macaque monkey visual cortex. *Proceedings of the Royal Society B*, *198*(1130), 1–59.

- Hughes, S. W., Lorincz, M., Cope, D. W., Blethyn, K. L., Kekesi, K. A., Parri, H. R., Juhasz, G., & Crunelli, V. (2004). Synchronized oscillations at alpha and theta frequencies in the lateral geniculate nucleus. *Neuron*, *42*(2), 253–268.
- Jones, E. G. (2000). Microcolumns in the cerebral cortex. *Proceedings of the National Academy of Sciences of the United States of America*, *97*(10), 5019–5021.
- Lachaux, J. P., Rodriguez, E., Martinerie, J., & Varela, F. J. (1999). Measuring phase synchrony in brain signals. *Human Brain Mapping*, *8*(4), 194–208.
- Lakatos, P., Karmos, G., Mehta, A. D., Ulbert, I., & Schroeder, C. E. (2008). Entrainment of neuronal oscillations as a mechanism of attentional selection. *Science*, *320*(5872), 110–113.
- Logothetis, N., Pauls, J., Bulthoff, H., & Poggio, T. (1994). View-dependent object recognition by monkeys. *Current Biology*, *4*(5), 401–414.
- Logothetis, N. K., Pauls, J., & Poggio, T. (1995). Shape representation in the inferior temporal cortex of monkeys. *Current Biology*, *5*(5), 552–563.
- Lopes da Silva, F. (1991). Neural mechanisms underlying brain waves: from neural membranes to networks. *Electroencephalography and Clinical Neurophysiology*, *79*(2), 81–93.
- Lorincz, M. L., Crunelli, V., & Hughes, S. W. (2008). Cellular dynamics of cholinergically induced alpha (8–13 Hz) rhythms in sensory thalamic nuclei in vitro. *The Journal of Neuroscience*, *28*(3), 660–671.
- Lorincz, M. L., Kekesi, K. A., Juhasz, G., Crunelli, V., & Hughes, S. W. (2009). Temporal framing of thalamic relay-mode firing by phasic inhibition during the alpha rhythm. *Neuron*, *63*(5), 683–696.
- Luczak, A., Bartho, P., & Harris, K. D. (2013). Gating of sensory input by spontaneous cortical activity. *The Journal of Neuroscience*, *33*(4), 1684–1695.
- Lumer, E., Edelman, G., & Tononi, G. (1997). Neural dynamics in a model of the thalamocortical system. I. Layers, loops and the emergence of fast synchronous rhythms. *Cerebral Cortex*, *7*(3), 207–227.
- Masquelier, T., & Thorpe, S. J. (2007). Unsupervised learning of visual features through spike timing dependent plasticity. *PLoS Computational Biology*, *3*(2), 247–257.
- Mathewson, K. E., Lleras, A., Beck, D. M., Fabiani, M., Ro, T., & Gratton, G. (2011). Pulsed out of awareness: EEG alpha oscillations represent a pulsed-inhibition of ongoing cortical processing. *Frontiers in Psychology*, *2*.
- Mountcastle, V. B. (1997). The columnar organization of the neocortex. *Brain*, *120*(Pt 4), 701–722.
- Mutch, J., & Lowe, D. (2008). Object class recognition and localization using sparse features with limited receptive fields. *International Journal of Computer Vision*, *80*(1), 45–57.
- Oostenveld, R., Fries, P., Maris, E., & Schoffelen, J.-M. (2011). FieldTrip: Open source software for advanced analysis of MEG, EEG, and invasive electrophysiological data. *Computational Intelligence and Neuroscience*, *2011*.
- O'Reilly, R. C., & Munakata, Y. (2000). *Computational Explorations in Cognitive Neuroscience: Understanding the Mind by Simulating the Brain*. Cambridge, MA: The MIT Press.

- O'Reilly, R. C., Munakata, Y., Frank, M. J., Hazy, T. E., & Contributors (2012). *Computational Cognitive Neuroscience*. Wiki Book, 1st Edition, URL: <http://ccnbook.colorado.edu>.
- Pelli, D. (1997). The VideoToolbox software for visual psychophysics: Transforming numbers into movies. *Spatial Vision*, 10(4), 437–442.
- Perrin, F., Pernier, J., Bertrand, O., & Echallier, J. F. (1989). Spherical splines for scalp potential and current density mapping. *Electroencephalography and Clinical Neurophysiology*, 72(2), 184–187.
- Rockland, K. S., & Pandya, D. N. (1979). Laminar origins and terminations of cortical connections of the occipital lobe in the rhesus monkey. *Brain Research*, 179(1), 3–20.
- Rohenkohl, G., & Nobre, A. C. (2011). Alpha oscillations related to anticipatory attention follow temporal expectations. *The Journal of Neuroscience*, 31(40), 14076–14084.
- Schroeder, C. E., & Lakatos, P. (2009). Low-frequency neuronal oscillations as instruments of sensory selection. *Trends in Neurosciences*, 32(1), 9–18.
- Serre, T., Oliva, A., & Poggio, T. (2007). A feedforward architecture accounts for rapid categorization. *Proceedings of the National Academy of Sciences of the United States of America*, 104(15), 6424–6429.
- Servan-Schreiber, D., Cleeremans, A., & McClelland, J. L. (1991). Graded state machines: The representation of temporal contingencies in simple recurrent networks. *Machine Learning*, 7(2–3), 161–193.
- Silva, L. R., Amitai, Y., & Connors, B. W. (1991). Intrinsic oscillations of neocortex generated by layer 5 pyramidal neurons. *Science*, 251(4992), 432–435.
- Sinha, P., & Poggio, T. (1996). Role of learning in three-dimensional form perception. *Nature*, 384(6608), 460–463.
- Spaak, E., Bonnefond, M., Maier, A., Leopold, D. A., & Jensen, O. (2012). Layer-specific entrainment of gamma-band neural activity by the alpha rhythm in monkey visual cortex. *Current Biology*, 22(24), 2313–2318.
- Stefanics, G., Hangya, B., Herndi, I., Winkler, I., Lakatos, P., & Ulbert, I. (2010). Phase entrainment of human delta oscillations can mediate the effects of expectation on reaction speed. *The Journal of Neuroscience*, 30(41), 13578–13585.
- Thomson, A. M. (2010). Neocortical layer 6, a review. *Frontiers in Neuroanatomy*, 4.
- Thomson, A. M., & Lamy, C. (2007). Functional maps of neocortical local circuitry. *Frontiers in Neuroscience*, 1(1), 19–42.
- Townshend, J. T., & Ashby, F. G. (1983). *Stochastic Modeling of Elementary Psychological Processes*. Cambridge: Cambridge University Press.
- Townshend, J. T., & Ashby, F. G. (2005). Methods of modeling capacity in simple processing systems. In J. N. Castellan Jr., & F. Restle (Eds.), *Cognitive Theory: Volume 3* (pp. 200–239). Hillsdale, NJ: Lawrence Erlbaum Associates.

- VanRullen, R., Busch, N. A., Drewes, J., & Dubois, J. (2011). Ongoing EEG phase as a trial-by-trial predictor of perceptual and attentional variability. *Frontiers in Psychology*, 2.
- Will, U., & Berg, E. (2007). Brain wave synchronization and entrainment to periodic acoustic stimuli. *Neuroscience letters*, 424(1), 55–60.

## **Chapter 5**

### **Neural model of spatial and temporal prediction for object recognition**

#### **5.1 Introduction**

TODO

#### **5.2 Methods**

##### **5.2.1 Model architecture**

##### **5.2.2 LeabraTI learning rule**

##### **5.2.3 Input environment**

#### **5.3 Results**

#### **5.4 Discussion**

#### **References**

- Armstrong-James, M., Fox, K., & Das-Gupta, A. (1992). Flow of excitation within rat barrel cortex on striking a single vibrissa. *Journal of Neurophysiology*, 68(4), 1345–1358.
- Arnal, L. H., & Giraud, A.-L. (2012). Cortical oscillations and sensory predictions. *Trends in Cognitive Sciences*, 16(7), 390–398.
- Balas, B. J., & Sinha, P. (2009). The role of sequence order in determining view canonicality for novel wire-frame objects. *Attention, Perception & Psychophysics*, 71(4), 712–723.
- Benjamini, Y., & Yekutieli, D. (2001). The control of the false discovery rate in multiple testing under dependency. *The Annals of Statistics*, 29(4), 1165–1188.
- Brainard, D. (1997). The Psychophysics Toolbox. *Spatial Vision*, 10(4), 433–436.

- Buffalo, E. A., Fries, P., Landman, R., Buschman, T. J., & Desimone, R. (2011). Laminar differences in gamma and alpha coherence in the ventral stream. *Proceedings of the National Academy of Sciences of the United States of America*, *108*(27), 11262–11267.
- Bulthoff, H. H., & Edelman, S. (1992). Psychophysical support for a two-dimensional view interpolation theory of object recognition. *Proceedings of the National Academy of Sciences of the United States of America*, *89*(1), 60–64.
- Busch, N. A., Dubois, J., & VanRullen, R. (2009). The phase of ongoing EEG oscillations predicts visual perception. *The Journal of Neuroscience*, *29*(24), 7869–7876.
- Buxhoeveden, D. P., & Casanova, M. F. (2002). The minicolumn hypothesis in neuroscience. *Brain*, *125*(Pt 5), 935–951.
- Connors, B. W., Gutnick, M. J., & Prince, D. A. (1982). Electrophysiological properties of neocortical neurons in vitro. *Journal of Neurophysiology*, *48*(6), 1302–1320.
- Cousineau, D. (2005). Confidence intervals in within-subject designs: A simpler solution to Loftus and Massons method. *Tutorials in Quantitative Methods for Psychology*, *1*(1), 42–45.
- Delorme, A., & Makeig, S. (2004). EEGLAB: An open source toolbox for analysis of single-trial EEG dynamics including independent component analysis. *Journal of Neuroscience Methods*, *134*(1), 9–21.
- Doherty, J. R., Rao, A., Mesulam, M. M., & Nobre, A. C. (2005). Synergistic effect of combined temporal and spatial expectations on visual attention. *The Journal of Neuroscience*, *25*(36), 8259–8266.
- Douglas, R. J., & Martin, K. A. C. (2004). Neuronal circuits of the neocortex. *Annual Review of Neuroscience*, *27*, 419–451.
- Edelman, S., & Bulthoff, H. H. (1992). Orientation dependence in the recognition of familiar and novel views of three-dimensional objects. *Vision Research*, *32*(12), 2385–2400.
- Elman, J. L. (1990). Finding structure in time. *Cognitive Science*, *14*(2), 179–211.
- Fahrenfort, J. J., Scholte, H. S., & Lamme, V. A. F. (2007). Masking disrupts reentrant processing in human visual cortex. *Journal of Cognitive Neuroscience*, *19*(9), 1488–1497.
- Felleman, D. J., & Van Essen, D. C. (1991). Distributed hierarchical processing in the primate cerebral cortex. *Cerebral Cortex*, *1*(1), 1–47.
- Foldiak, P. (1991). Learning invariance from transformation sequences. *Neural Computation*, *3*(2), 194–200.
- Franceschetti, S., Guatteo, E., Panzica, F., Sancini, G., Wanke, E., & Avanzini, G. (1995). Ionic mechanisms underlying burst firing in pyramidal neurons: Intracellular study in rat sensorimotor cortex. *Brain Research*, *696*(1–2), 127–139.
- Giraud, A.-L., & Poeppel, D. (2012). Cortical oscillations and speech processing: Emerging computational principles and operations. *Nature Neuroscience*, *15*(4), 511–517.
- Hirsch, J. A., & Martinez, L. M. (2006). Laminar processing in the visual cortical column. *Current Opinion in Neurobiology*, *16*(4), 377–384.

- Horton, J. C., & Adams, D. L. (2005). The cortical column: A structure without a function. *Philosophical Transactions of the Royal Society B*, *360*(1456), 837–862.
- Hubel, D. H., & Wiesel, T. N. (1977). Ferrier lecture. Functional architecture of macaque monkey visual cortex. *Proceedings of the Royal Society B*, *198*(1130), 1–59.
- Hughes, S. W., Lorincz, M., Cope, D. W., Blethyn, K. L., Kekesi, K. A., Parri, H. R., Juhasz, G., & Crunelli, V. (2004). Synchronized oscillations at alpha and theta frequencies in the lateral geniculate nucleus. *Neuron*, *42*(2), 253–268.
- Jones, E. G. (2000). Microcolumns in the cerebral cortex. *Proceedings of the National Academy of Sciences of the United States of America*, *97*(10), 5019–5021.
- Lachaux, J. P., Rodriguez, E., Martinerie, J., & Varela, F. J. (1999). Measuring phase synchrony in brain signals. *Human Brain Mapping*, *8*(4), 194–208.
- Lakatos, P., Karmos, G., Mehta, A. D., Ulbert, I., & Schroeder, C. E. (2008). Entrainment of neuronal oscillations as a mechanism of attentional selection. *Science*, *320*(5872), 110–113.
- Logothetis, N., Pauls, J., Bulthoff, H., & Poggio, T. (1994). View-dependent object recognition by monkeys. *Current Biology*, *4*(5), 401–414.
- Logothetis, N. K., Pauls, J., & Poggio, T. (1995). Shape representation in the inferior temporal cortex of monkeys. *Current Biology*, *5*(5), 552–563.
- Lopes da Silva, F. (1991). Neural mechanisms underlying brain waves: from neural membranes to networks. *Electroencephalography and Clinical Neurophysiology*, *79*(2), 81–93.
- Lorincz, M. L., Crunelli, V., & Hughes, S. W. (2008). Cellular dynamics of cholinergically induced alpha (8–13 hz) rhythms in sensory thalamic nuclei in vitro. *The Journal of Neuroscience*, *28*(3), 660–671.
- Lorincz, M. L., Kekesi, K. A., Juhasz, G., Crunelli, V., & Hughes, S. W. (2009). Temporal framing of thalamic relay-mode firing by phasic inhibition during the alpha rhythm. *Neuron*, *63*(5), 683–696.
- Luczak, A., Bartho, P., & Harris, K. D. (2013). Gating of sensory input by spontaneous cortical activity. *The Journal of Neuroscience*, *33*(4), 1684–1695.
- Lumer, E., Edelman, G., & Tononi, G. (1997). Neural dynamics in a model of the thalamocortical system. I. Layers, loops and the emergence of fast synchronous rhythms. *Cerebral Cortex*, *7*(3), 207–227.
- Masquelier, T., & Thorpe, S. J. (2007). Unsupervised learning of visual features through spike timing dependent plasticity. *PLoS Computational Biology*, *3*(2), 247–257.
- Mathewson, K. E., Lleras, A., Beck, D. M., Fabiani, M., Ro, T., & Gratton, G. (2011). Pulsed out of awareness: EEG alpha oscillations represent a pulsed-inhibition of ongoing cortical processing. *Frontiers in Psychology*, *2*.
- Mountcastle, V. B. (1997). The columnar organization of the neocortex. *Brain*, *120*(Pt 4), 701–722.
- Mutch, J., & Lowe, D. (2008). Object class recognition and localization using sparse features with limited receptive fields. *International Journal of Computer Vision*, *80*(1), 45–57.

- Oostenveld, R., Fries, P., Maris, E., & Schoffelen, J.-M. (2011). FieldTrip: Open source software for advanced analysis of MEG, EEG, and invasive electrophysiological data. *Computational Intelligence and Neuroscience*, 2011.
- O'Reilly, R. C., & Munakata, Y. (2000). *Computational Explorations in Cognitive Neuroscience: Understanding the Mind by Simulating the Brain*. Cambridge, MA: The MIT Press.
- O'Reilly, R. C., Munakata, Y., Frank, M. J., Hazy, T. E., & Contributors (2012). *Computational Cognitive Neuroscience*. Wiki Book, 1st Edition, URL: <http://ccnbook.colorado.edu>.
- Pelli, D. (1997). The VideoToolbox software for visual psychophysics: Transforming numbers into movies. *Spatial Vision*, 10(4), 437–442.
- Perrin, F., Pernier, J., Bertrand, O., & Echallier, J. F. (1989). Spherical splines for scalp potential and current density mapping. *Electroencephalography and Clinical Neurophysiology*, 72(2), 184–187.
- Rockland, K. S., & Pandya, D. N. (1979). Laminar origins and terminations of cortical connections of the occipital lobe in the rhesus monkey. *Brain Research*, 179(1), 3–20.
- Rohenkohl, G., & Nobre, A. C. (2011). Alpha oscillations related to anticipatory attention follow temporal expectations. *The Journal of Neuroscience*, 31(40), 14076–14084.
- Schroeder, C. E., & Lakatos, P. (2009). Low-frequency neuronal oscillations as instruments of sensory selection. *Trends in Neurosciences*, 32(1), 9–18.
- Serre, T., Oliva, A., & Poggio, T. (2007). A feedforward architecture accounts for rapid categorization. *Proceedings of the National Academy of Sciences of the United States of America*, 104(15), 6424–6429.
- Servan-Schreiber, D., Cleeremans, A., & McClelland, J. L. (1991). Graded state machines: The representation of temporal contingencies in simple recurrent networks. *Machine Learning*, 7(2–3), 161–193.
- Silva, L. R., Amitai, Y., & Connors, B. W. (1991). Intrinsic oscillations of neocortex generated by layer 5 pyramidal neurons. *Science*, 251(4992), 432–435.
- Sinha, P., & Poggio, T. (1996). Role of learning in three-dimensional form perception. *Nature*, 384(6608), 460–463.
- Spaak, E., Bonnefond, M., Maier, A., Leopold, D. A., & Jensen, O. (2012). Layer-specific entrainment of gamma-band neural activity by the alpha rhythm in monkey visual cortex. *Current Biology*, 22(24), 2313–2318.
- Stefanics, G., Hangya, B., Herndi, I., Winkler, I., Lakatos, P., & Ulbert, I. (2010). Phase entrainment of human delta oscillations can mediate the effects of expectation on reaction speed. *The Journal of Neuroscience*, 30(41), 13578–13585.
- Thomson, A. M. (2010). Neocortical layer 6, a review. *Frontiers in Neuroanatomy*, 4.
- Thomson, A. M., & Lamy, C. (2007). Functional maps of neocortical local circuitry. *Frontiers in Neuroscience*, 1(1), 19–42.

- Townshend, J. T., & Ashby, F. G. (1983). Stochastic Modeling of Elementary Psychological Processes. Cambridge: Cambridge University Press.
- Townshend, J. T., & Ashby, F. G. (2005). Methods of modeling capacity in simple processing systems. In J. N. Castellan Jr., & F. Restle (Eds.), Cognitive Theory: Volume 3 (pp. 200–239). Hillsdale, NJ: Lawrence Erlbaum Associates.
- VanRullen, R., Busch, N. A., Drewes, J., & Dubois, J. (2011). Ongoing EEG phase as a trial-by-trial predictor of perceptual and attentional variability. Frontiers in Psychology, 2.
- Will, U., & Berg, E. (2007). Brain wave synchronization and entrainment to periodic acoustic stimuli. Neuroscience letters, 424(1), 55–60.

## **Chapter 6**

### **General Discussion**

### **References**

- Armstrong-James, M., Fox, K., & Das-Gupta, A. (1992). Flow of excitation within rat barrel cortex on striking a single vibrissa. *Journal of Neurophysiology*, *68*(4), 1345–1358.
- Arnal, L. H., & Giraud, A.-L. (2012). Cortical oscillations and sensory predictions. *Trends in Cognitive Sciences*, *16*(7), 390–398.
- Balas, B. J., & Sinha, P. (2009). The role of sequence order in determining view canonicality for novel wire-frame objects. *Attention, Perception & Psychophysics*, *71*(4), 712–723.
- Benjamini, Y., & Yekutieli, D. (2001). The control of the false discovery rate in multiple testing under dependency. *The Annals of Statistics*, *29*(4), 1165–1188.
- Brainard, D. (1997). The Psychophysics Toolbox. *Spatial Vision*, *10*(4), 433–436.
- Buffalo, E. A., Fries, P., Landman, R., Buschman, T. J., & Desimone, R. (2011). Laminar differences in gamma and alpha coherence in the ventral stream. *Proceedings of the National Academy of Sciences of the United States of America*, *108*(27), 11262–11267.
- Bulthoff, H. H., & Edelman, S. (1992). Psychophysical support for a two-dimensional view interpolation theory of object recognition. *Proceedings of the National Academy of Sciences of the United States of America*, *89*(1), 60–64.
- Busch, N. A., Dubois, J., & VanRullen, R. (2009). The phase of ongoing EEG oscillations predicts visual perception. *The Journal of Neuroscience*, *29*(24), 7869–7876.
- Buxhoeveden, D. P., & Casanova, M. F. (2002). The minicolumn hypothesis in neuroscience. *Brain*, *125*(Pt 5), 935–951.
- Connors, B. W., Gutnick, M. J., & Prince, D. A. (1982). Electrophysiological properties of neocortical neurons in vitro. *Journal of Neurophysiology*, *48*(6), 1302–1320.
- Cousineau, D. (2005). Confidence intervals in within-subject designs: A simpler solution to Loftus and Massons method. *Tutorials in Quantitative Methods for Psychology*, *1*(1), 42–45.
- Delorme, A., & Makeig, S. (2004). EEGLAB: An open source toolbox for analysis of single-trial EEG dynamics including independent component analysis. *Journal of Neuroscience Methods*, *134*(1), 9–21.

- Doherty, J. R., Rao, A., Mesulam, M. M., & Nobre, A. C. (2005). Synergistic effect of combined temporal and spatial expectations on visual attention. *The Journal of Neuroscience*, *25*(36), 8259–8266.
- Douglas, R. J., & Martin, K. A. C. (2004). Neuronal circuits of the neocortex. *Annual Review of Neuroscience*, *27*, 419–451.
- Edelman, S., & Bulthoff, H. H. (1992). Orientation dependence in the recognition of familiar and novel views of three-dimensional objects. *Vision Research*, *32*(12), 2385–2400.
- Elman, J. L. (1990). Finding structure in time. *Cognitive Science*, *14*(2), 179–211.
- Fahrenfort, J. J., Scholte, H. S., & Lamme, V. A. F. (2007). Masking disrupts reentrant processing in human visual cortex. *Journal of Cognitive Neuroscience*, *19*(9), 1488–1497.
- Felleman, D. J., & Van Essen, D. C. (1991). Distributed hierarchical processing in the primate cerebral cortex. *Cerebral Cortex*, *1*(1), 1–47.
- Foldiak, P. (1991). Learning invariance from transformation sequences. *Neural Computation*, *3*(2), 194–200.
- Franceschetti, S., Guatteo, E., Panzica, F., Sancini, G., Wanke, E., & Avanzini, G. (1995). Ionic mechanisms underlying burst firing in pyramidal neurons: Intracellular study in rat sensorimotor cortex. *Brain Research*, *696*(1–2), 127–139.
- Giraud, A.-L., & Poeppel, D. (2012). Cortical oscillations and speech processing: Emerging computational principles and operations. *Nature Neuroscience*, *15*(4), 511–517.
- Hirsch, J. A., & Martinez, L. M. (2006). Laminar processing in the visual cortical column. *Current Opinion in Neurobiology*, *16*(4), 377–384.
- Horton, J. C., & Adams, D. L. (2005). The cortical column: A structure without a function. *Philosophical Transactions of the Royal Society B*, *360*(1456), 837–862.
- Hubel, D. H., & Wiesel, T. N. (1977). Ferrier lecture. Functional architecture of macaque monkey visual cortex. *Proceedings of the Royal Society B*, *198*(1130), 1–59.
- Hughes, S. W., Lorincz, M., Cope, D. W., Blethyn, K. L., Kekesi, K. A., Parri, H. R., Juhasz, G., & Crunelli, V. (2004). Synchronized oscillations at alpha and theta frequencies in the lateral geniculate nucleus. *Neuron*, *42*(2), 253–268.
- Jones, E. G. (2000). Microcolumns in the cerebral cortex. *Proceedings of the National Academy of Sciences of the United States of America*, *97*(10), 5019–5021.
- Lachaux, J. P., Rodriguez, E., Martinerie, J., & Varela, F. J. (1999). Measuring phase synchrony in brain signals. *Human Brain Mapping*, *8*(4), 194–208.
- Lakatos, P., Karmos, G., Mehta, A. D., Ulbert, I., & Schroeder, C. E. (2008). Entrainment of neuronal oscillations as a mechanism of attentional selection. *Science*, *320*(5872), 110–113.
- Logothetis, N., Pauls, J., Bulthoff, H., & Poggio, T. (1994). View-dependent object recognition by monkeys. *Current Biology*, *4*(5), 401–414.
- Logothetis, N. K., Pauls, J., & Poggio, T. (1995). Shape representation in the inferior temporal cortex of monkeys. *Current Biology*, *5*(5), 552–563.

- Lopes da Silva, F. (1991). Neural mechanisms underlying brain waves: from neural membranes to networks. *Electroencephalography and Clinical Neurophysiology*, 79(2), 81–93.
- Lorincz, M. L., Crunelli, V., & Hughes, S. W. (2008). Cellular dynamics of cholinergically induced alpha (8–13 hz) rhythms in sensory thalamic nuclei in vitro. *The Journal of Neuroscience*, 28(3), 660–671.
- Lorincz, M. L., Kekesi, K. A., Juhasz, G., Crunelli, V., & Hughes, S. W. (2009). Temporal framing of thalamic relay-mode firing by phasic inhibition during the alpha rhythm. *Neuron*, 63(5), 683–696.
- Luczak, A., Bartho, P., & Harris, K. D. (2013). Gating of sensory input by spontaneous cortical activity. *The Journal of Neuroscience*, 33(4), 1684–1695.
- Lumer, E., Edelman, G., & Tononi, G. (1997). Neural dynamics in a model of the thalamocortical system. I. Layers, loops and the emergence of fast synchronous rhythms. *Cerebral Cortex*, 7(3), 207–227.
- Masquelier, T., & Thorpe, S. J. (2007). Unsupervised learning of visual features through spike timing dependent plasticity. *PLoS Computational Biology*, 3(2), 247–257.
- Mathewson, K. E., Lleras, A., Beck, D. M., Fabiani, M., Ro, T., & Gratton, G. (2011). Pulsed out of awareness: EEG alpha oscillations represent a pulsed-inhibition of ongoing cortical processing. *Frontiers in Psychology*, 2.
- Mountcastle, V. B. (1997). The columnar organization of the neocortex. *Brain*, 120(Pt 4), 701–722.
- Mutch, J., & Lowe, D. (2008). Object class recognition and localization using sparse features with limited receptive fields. *International Journal of Computer Vision*, 80(1), 45–57.
- Oostenveld, R., Fries, P., Maris, E., & Schoffelen, J.-M. (2011). FieldTrip: Open source software for advanced analysis of MEG, EEG, and invasive electrophysiological data. *Computational Intelligence and Neuroscience*, 2011.
- O'Reilly, R. C., & Munakata, Y. (2000). *Computational Explorations in Cognitive Neuroscience: Understanding the Mind by Simulating the Brain*. Cambridge, MA: The MIT Press.
- O'Reilly, R. C., Munakata, Y., Frank, M. J., Hazy, T. E., & Contributors (2012). *Computational Cognitive Neuroscience*. Wiki Book, 1st Edition, URL: <http://ccnbook.colorado.edu>.
- Pelli, D. (1997). The VideoToolbox software for visual psychophysics: Transforming numbers into movies. *Spatial Vision*, 10(4), 437–442.
- Perrin, F., Pernier, J., Bertrand, O., & Echallier, J. F. (1989). Spherical splines for scalp potential and current density mapping. *Electroencephalography and Clinical Neurophysiology*, 72(2), 184–187.
- Rockland, K. S., & Pandya, D. N. (1979). Laminar origins and terminations of cortical connections of the occipital lobe in the rhesus monkey. *Brain Research*, 179(1), 3–20.
- Rohenkohl, G., & Nobre, A. C. (2011). Alpha oscillations related to anticipatory attention follow temporal expectations. *The Journal of Neuroscience*, 31(40), 14076–14084.

- Schroeder, C. E., & Lakatos, P. (2009). Low-frequency neuronal oscillations as instruments of sensory selection. *Trends in Neurosciences*, *32*(1), 9–18.
- Serre, T., Oliva, A., & Poggio, T. (2007). A feedforward architecture accounts for rapid categorization. *Proceedings of the National Academy of Sciences of the United States of America*, *104*(15), 6424–6429.
- Servan-Schreiber, D., Cleeremans, A., & McClelland, J. L. (1991). Graded state machines: The representation of temporal contingencies in simple recurrent networks. *Machine Learning*, *7*(2–3), 161–193.
- Silva, L. R., Amitai, Y., & Connors, B. W. (1991). Intrinsic oscillations of neocortex generated by layer 5 pyramidal neurons. *Science*, *251*(4992), 432–435.
- Sinha, P., & Poggio, T. (1996). Role of learning in three-dimensional form perception. *Nature*, *384*(6608), 460–463.
- Spaak, E., Bonnefond, M., Maier, A., Leopold, D. A., & Jensen, O. (2012). Layer-specific entrainment of gamma-band neural activity by the alpha rhythm in monkey visual cortex. *Current Biology*, *22*(24), 2313–2318.
- Stefanics, G., Hangya, B., Herndi, I., Winkler, I., Lakatos, P., & Ulbert, I. (2010). Phase entrainment of human delta oscillations can mediate the effects of expectation on reaction speed. *The Journal of Neuroscience*, *30*(41), 13578–13585.
- Thomson, A. M. (2010). Neocortical layer 6, a review. *Frontiers in Neuroanatomy*, *4*.
- Thomson, A. M., & Lamy, C. (2007). Functional maps of neocortical local circuitry. *Frontiers in Neuroscience*, *1*(1), 19–42.
- Townshend, J. T., & Ashby, F. G. (1983). *Stochastic Modeling of Elementary Psychological Processes*. Cambridge: Cambridge University Press.
- Townshend, J. T., & Ashby, F. G. (2005). Methods of modeling capacity in simple processing systems. In J. N. Castellan Jr., & F. Restle (Eds.), *Cognitive Theory: Volume 3* (pp. 200–239). Hillsdale, NJ: Lawrence Erlbaum Associates.
- VanRullen, R., Busch, N. A., Drewes, J., & Dubois, J. (2011). Ongoing EEG phase as a trial-by-trial predictor of perceptual and attentional variability. *Frontiers in Psychology*, *2*.
- Will, U., & Berg, E. (2007). Brain wave synchronization and entrainment to periodic acoustic stimuli. *Neuroscience letters*, *424*(1), 55–60.

## References

- Armstrong-James, M., Fox, K., & Das-Gupta, A. (1992). Flow of excitation within rat barrel cortex on striking a single vibrissa. *Journal of Neurophysiology*, *68*(4), 1345–1358.
- Arnal, L. H., & Giraud, A.-L. (2012). Cortical oscillations and sensory predictions. *Trends in Cognitive Sciences*, *16*(7), 390–398.

- Balas, B. J., & Sinha, P. (2009). The role of sequence order in determining view canonicality for novel wire-frame objects. *Attention, Perception & Psychophysics*, *71*(4), 712–723.
- Benjamini, Y., & Yekutieli, D. (2001). The control of the false discovery rate in multiple testing under dependency. *The Annals of Statistics*, *29*(4), 1165–1188.
- Brainard, D. (1997). The Psychophysics Toolbox. *Spatial Vision*, *10*(4), 433–436.
- Buffalo, E. A., Fries, P., Landman, R., Buschman, T. J., & Desimone, R. (2011). Laminar differences in gamma and alpha coherence in the ventral stream. *Proceedings of the National Academy of Sciences of the United States of America*, *108*(27), 11262–11267.
- Bulthoff, H. H., & Edelman, S. (1992). Psychophysical support for a two-dimensional view interpolation theory of object recognition. *Proceedings of the National Academy of Sciences of the United States of America*, *89*(1), 60–64.
- Busch, N. A., Dubois, J., & VanRullen, R. (2009). The phase of ongoing EEG oscillations predicts visual perception. *The Journal of Neuroscience*, *29*(24), 7869–7876.
- Buxhoeveden, D. P., & Casanova, M. F. (2002). The minicolumn hypothesis in neuroscience. *Brain*, *125*(Pt 5), 935–951.
- Connors, B. W., Gutnick, M. J., & Prince, D. A. (1982). Electrophysiological properties of neocortical neurons in vitro. *Journal of Neurophysiology*, *48*(6), 1302–1320.
- Cousineau, D. (2005). Confidence intervals in within-subject designs: A simpler solution to Loftus and Massons method. *Tutorials in Quantitative Methods for Psychology*, *1*(1), 42–45.
- Delorme, A., & Makeig, S. (2004). EEGLAB: An open source toolbox for analysis of single-trial EEG dynamics including independent component analysis. *Journal of Neuroscience Methods*, *134*(1), 9–21.
- Doherty, J. R., Rao, A., Mesulam, M. M., & Nobre, A. C. (2005). Synergistic effect of combined temporal and spatial expectations on visual attention. *The Journal of Neuroscience*, *25*(36), 8259–8266.
- Douglas, R. J., & Martin, K. A. C. (2004). Neuronal circuits of the neocortex. *Annual Review of Neuroscience*, *27*, 419–451.
- Edelman, S., & Bulthoff, H. H. (1992). Orientation dependence in the recognition of familiar and novel views of three-dimensional objects. *Vision Research*, *32*(12), 2385–2400.
- Elman, J. L. (1990). Finding structure in time. *Cognitive Science*, *14*(2), 179–211.
- Fahrenfort, J. J., Scholte, H. S., & Lamme, V. A. F. (2007). Masking disrupts reentrant processing in human visual cortex. *Journal of Cognitive Neuroscience*, *19*(9), 1488–1497.
- Felleman, D. J., & Van Essen, D. C. (1991). Distributed hierarchical processing in the primate cerebral cortex. *Cerebral Cortex*, *1*(1), 1–47.
- Foldiak, P. (1991). Learning invariance from transformation sequences. *Neural Computation*, *3*(2), 194–200.
- Franceschetti, S., Guatteo, E., Panzica, F., Sancini, G., Wanke, E., & Avanzini, G. (1995). Ionic mechanisms underlying burst firing in pyramidal neurons: Intracellular study in rat sensorimotor cortex. *Brain Research*, *696*(1–2), 127–139.

- Giraud, A.-L., & Poeppel, D. (2012). Cortical oscillations and speech processing: Emerging computational principles and operations. *Nature Neuroscience*, *15*(4), 511–517.
- Hirsch, J. A., & Martinez, L. M. (2006). Laminar processing in the visual cortical column. *Current Opinion in Neurobiology*, *16*(4), 377–384.
- Horton, J. C., & Adams, D. L. (2005). The cortical column: A structure without a function. *Philosophical Transactions of the Royal Society B*, *360*(1456), 837–862.
- Hubel, D. H., & Wiesel, T. N. (1977). Ferrier lecture. Functional architecture of macaque monkey visual cortex. *Proceedings of the Royal Society B*, *198*(1130), 1–59.
- Hughes, S. W., Lorincz, M., Cope, D. W., Blethyn, K. L., Kekesi, K. A., Parri, H. R., Juhasz, G., & Crunelli, V. (2004). Synchronized oscillations at alpha and theta frequencies in the lateral geniculate nucleus. *Neuron*, *42*(2), 253–268.
- Jones, E. G. (2000). Microcolumns in the cerebral cortex. *Proceedings of the National Academy of Sciences of the United States of America*, *97*(10), 5019–5021.
- Lachaux, J. P., Rodriguez, E., Martinerie, J., & Varela, F. J. (1999). Measuring phase synchrony in brain signals. *Human Brain Mapping*, *8*(4), 194–208.
- Lakatos, P., Karmos, G., Mehta, A. D., Ulbert, I., & Schroeder, C. E. (2008). Entrainment of neuronal oscillations as a mechanism of attentional selection. *Science*, *320*(5872), 110–113.
- Logothetis, N., Pauls, J., Bulthoff, H., & Poggio, T. (1994). View-dependent object recognition by monkeys. *Current Biology*, *4*(5), 401–414.
- Logothetis, N. K., Pauls, J., & Poggio, T. (1995). Shape representation in the inferior temporal cortex of monkeys. *Current Biology*, *5*(5), 552–563.
- Lopes da Silva, F. (1991). Neural mechanisms underlying brain waves: from neural membranes to networks. *Electroencephalography and Clinical Neurophysiology*, *79*(2), 81–93.
- Lorincz, M. L., Crunelli, V., & Hughes, S. W. (2008). Cellular dynamics of cholinergically induced alpha (8–13 Hz) rhythms in sensory thalamic nuclei in vitro. *The Journal of Neuroscience*, *28*(3), 660–671.
- Lorincz, M. L., Kekesi, K. A., Juhasz, G., Crunelli, V., & Hughes, S. W. (2009). Temporal framing of thalamic relay-mode firing by phasic inhibition during the alpha rhythm. *Neuron*, *63*(5), 683–696.
- Luczak, A., Bartho, P., & Harris, K. D. (2013). Gating of sensory input by spontaneous cortical activity. *The Journal of Neuroscience*, *33*(4), 1684–1695.
- Lumer, E., Edelman, G., & Tononi, G. (1997). Neural dynamics in a model of the thalamocortical system. I. Layers, loops and the emergence of fast synchronous rhythms. *Cerebral Cortex*, *7*(3), 207–227.
- Masquelier, T., & Thorpe, S. J. (2007). Unsupervised learning of visual features through spike timing dependent plasticity. *PLoS Computational Biology*, *3*(2), 247–257.
- Mathewson, K. E., Lleras, A., Beck, D. M., Fabiani, M., Ro, T., & Gratton, G. (2011). Pulsed out of awareness: EEG alpha oscillations represent a pulsed-inhibition of ongoing cortical processing. *Frontiers in Psychology*, *2*.

- Mountcastle, V. B. (1997). The columnar organization of the neocortex. *Brain*, *120*(Pt 4), 701–722.
- Mutch, J., & Lowe, D. (2008). Object class recognition and localization using sparse features with limited receptive fields. *International Journal of Computer Vision*, *80*(1), 45–57.
- Oostenveld, R., Fries, P., Maris, E., & Schoffelen, J.-M. (2011). FieldTrip: Open source software for advanced analysis of MEG, EEG, and invasive electrophysiological data. *Computational Intelligence and Neuroscience*, *2011*.
- O'Reilly, R. C., & Munakata, Y. (2000). *Computational Explorations in Cognitive Neuroscience: Understanding the Mind by Simulating the Brain*. Cambridge, MA: The MIT Press.
- O'Reilly, R. C., Munakata, Y., Frank, M. J., Hazy, T. E., & Contributors (2012). *Computational Cognitive Neuroscience*. Wiki Book, 1st Edition, URL: <http://ccnbook.colorado.edu>.
- Pelli, D. (1997). The VideoToolbox software for visual psychophysics: Transforming numbers into movies. *Spatial Vision*, *10*(4), 437–442.
- Perrin, F., Pernier, J., Bertrand, O., & Echallier, J. F. (1989). Spherical splines for scalp potential and current density mapping. *Electroencephalography and Clinical Neurophysiology*, *72*(2), 184–187.
- Rockland, K. S., & Pandya, D. N. (1979). Laminar origins and terminations of cortical connections of the occipital lobe in the rhesus monkey. *Brain Research*, *179*(1), 3–20.
- Rohenkohl, G., & Nobre, A. C. (2011). Alpha oscillations related to anticipatory attention follow temporal expectations. *The Journal of Neuroscience*, *31*(40), 14076–14084.
- Schroeder, C. E., & Lakatos, P. (2009). Low-frequency neuronal oscillations as instruments of sensory selection. *Trends in Neurosciences*, *32*(1), 9–18.
- Serre, T., Oliva, A., & Poggio, T. (2007). A feedforward architecture accounts for rapid categorization. *Proceedings of the National Academy of Sciences of the United States of America*, *104*(15), 6424–6429.
- Servan-Schreiber, D., Cleeremans, A., & McClelland, J. L. (1991). Graded state machines: The representation of temporal contingencies in simple recurrent networks. *Machine Learning*, *7*(2–3), 161–193.
- Silva, L. R., Amitai, Y., & Connors, B. W. (1991). Intrinsic oscillations of neocortex generated by layer 5 pyramidal neurons. *Science*, *251*(4992), 432–435.
- Sinha, P., & Poggio, T. (1996). Role of learning in three-dimensional form perception. *Nature*, *384*(6608), 460–463.
- Spaak, E., Bonnefond, M., Maier, A., Leopold, D. A., & Jensen, O. (2012). Layer-specific entrainment of gamma-band neural activity by the alpha rhythm in monkey visual cortex. *Current Biology*, *22*(24), 2313–2318.
- Stefanics, G., Hangya, B., Herndi, I., Winkler, I., Lakatos, P., & Ulbert, I. (2010). Phase entrainment of human delta oscillations can mediate the effects of expectation on reaction speed. *The Journal of Neuroscience*, *30*(41), 13578–13585.
- Thomson, A. M. (2010). Neocortical layer 6, a review. *Frontiers in Neuroanatomy*, *4*.

- Thomson, A. M., & Lamy, C. (2007). Functional maps of neocortical local circuitry. *Frontiers in Neuroscience*, 1(1), 19–42.
- Townshend, J. T., & Ashby, F. G. (1983). *Stochastic Modeling of Elementary Psychological Processes*. Cambridge: Cambridge University Press.
- Townshend, J. T., & Ashby, F. G. (2005). Methods of modeling capacity in simple processing systems. In J. N. Castellan Jr., & F. Restle (Eds.), *Cognitive Theory: Volume 3* (pp. 200–239). Hillsdale, NJ: Lawrence Erlbaum Associates.
- VanRullen, R., Busch, N. A., Drewes, J., & Dubois, J. (2011). Ongoing EEG phase as a trial-by-trial predictor of perceptual and attentional variability. *Frontiers in Psychology*, 2.
- Will, U., & Berg, E. (2007). Brain wave synchronization and entrainment to periodic acoustic stimuli. *Neuroscience letters*, 424(1), 55–60.